The Development and Evaluation of a Contractile, Hydrogel Scaffold for Skeletal Muscle Tissue Engineering

By

AMIN KHALILI

A thesis submitted to the

School of Graduate Studies

Rutgers, The State University of New Jersey

In partial fulfillment of the requirements

For the degree of

Master of Science

Graduate Program in Biomedical Engineering

Written under the direction of

Joseph W. Freeman, Ph.D.

And approved by

_____

_____

_____

New Brunswick, New Jersey

May 2020

ABSTRACT OF THE THESIS

The Development and Evaluation of a Contractile, Hydrogel Scaffold for Skeletal Muscle Tissue Engineering

By AMIN KHALILI

Thesis Director:

Joseph W. Freeman, Ph.D.

Skeletal muscle tissue has the ability to regenerate and return function to the damaged areas following an incident that has resulted in muscle loss or injury. However, in severe injuries with large volumetric deficiencies, body's natural healing mechanisms fall short and require artificial interventions. There currently exist surgical treatments such as muscle flaps to promote healing and help damaged skeletal muscle tissue to return to their functional state. However, such treatments have significant drawbacks and often lead to a lowered quality life for patients. The field of tissue engineering has demonstrated preliminary advances through the use of three-dimensional scaffolds as a solution to develop a personalized treatment for volumetric muscle loss. Despite such advances in this field, there remains an abundant of hurdles before scaffolds can become widely used in clinical setting. Recently tissue engineers have been successful to design skeletal muscle scaffolds that led to the fusion of myoblasts into myotubes, however, the lack of electrical and mechanical stimuli similar to the native tissue can prevent the formation of functional muscle. The overall goal of this research project is to develop polymeric scaffolds to deliver the necessary stimuli to form functional skeletal muscles. Herein, Poly(ethylene glycol) diacrylate (PEGDA) has been copolymerized with MAETAC to form an electroactive

polymer, that can change size or shape as a response to an electric field, has been combined with PEDOT:PSS to develop a skeletal muscle tissue engineering scaffold. To that end, this project has the following aims: 1) Characterize and optimize a positively charged poly(ethylene glycol) diacrylate based hydrogel as an actuating muscle tissue engineering scaffold; 2) Develop and optimize an electroconductive self-actuating multilayer scaffold for skeletal muscle tissue engineering.

Acknowledgement

As with every project, there exists many people that have contributed to growth and progress of this work. However, I would like to begin by thanking my amazing thesis advisor Dr. Joseph Freeman for believing in me and providing unconditional guidance throughout the project. Thank you for inspiring us every day and seeing our strengths and not our weaknesses. After every meeting I felt more confident in moving forward and do the work that brought me about writing this thesis.

To Dr. Labazzo and Dr. Olabisi, thank you so much for being on my committee, all your kind advice, feedback, flexibility, and most importantly your time.

I would also like to thank Mike Pellegrini, for spending countless hours helping and patiently me teaching various techniques used in developing this project. You are such an amazing, kind, and intelligent individual and I am very happy to have worked with you for the past two years. Lastly, I would like to thank my fellow coworkers for your feedback, encouragement, and assistant throughout the course of this project. My fellow coworker's past and present including Dr. Daniel Browe, Sonal Gahlawat, Xin Liu, Fernando Rebolledo, Brandon Newton, Hudifah Rabie, and Christian Buckley have all been amazing friends.

Additionally, I would like to thank Lawrence Stromberg for not only being an amazing graduate administrator that our department certainly cannot survive without, but also for all the advice, support, and kindness.

I would also like to thank my dear parents and my sister for the constant love and support throughout the years.

Lastl, I want to not only thank my lovely fiancée, Maryam Shanehsaz, for her support and unconditional love, but also to dedicate this piece of work to her.

TABLE OF CONTENTS

ABSTRACT…… ii

ACKNOWLEDGEMENTS..... iv

TABLE OF CONTENTS..... vi

CHAPTER 1: Background and Introduction……..……. 1

1.1 Skeletal Muscle Anatomy and Physiology……... 1

1.2 Skeletal Muscle Tissue Engineering …….……..……..... 5

1.3 Electroactive polymers and Artificial Muscles for Skeletal Muscle Tissue Engineering……...……..…….. 8

1.4 Project Goal and Specific Aims…… 10

1.5 References……11

CHAPTER 2: Characterization and Optimization of a Positively Charged Poly(Ethylene Glycol) Diacrylate Hydrogel as an Actuating Muscle Tissue Engineering Scaffold..... 15

2.1 Abstract……..... 15

2.2 Introduction…….……..15

2.3 Materials and Methods……. 17

2.3.1 Hydrogel Preparation and Swelling ……... 17

2.3.2 FTIR Spectroscopy…….. 19

2.3.3 Actuation Tests……...……. 29

2.3.4 Effect of Solution Ions on Actuation…….……. 20

2.3.5 Contractile Strength …… 21

2.3.6 Polymer Biocompatibility ……...22

2.3.7 Statistics……22

2.4 Results……... 23

2.4.1 FTIR Spectroscopy ……..……... 23

2.4.2 The Effects of Varying the Molecular Weight of PEGDA……..24

2.4.3 The Effects of Varying the Concentrations of MAETAC and PEGDA.. 24

2.4.4 The Effects of Varying Hydrogel Thickness……..…. 28

2.4.5 Contractile Strength……. 29

2.4.6 C2C12 Cytotoxicity Study……..……...……..30

2.5 Discussion…….32

2.6 Conclusion…… 36

2.7 References…….37

CHAPTER 3: Self-Actuating Multilayer Scaffold for Skeletal Muscle Tissue Engineering…… 39

3.1 Abstract….……... 39

3.2 Introduction…….……..39

3.3 Experimental Section…….42

3.3.1 Materials…….42

3.3.2 PEDOT:PSS/GO Nanocomposite Film Fabrication ……....42

3.3.3 Self-Actuating Multilayer Scaffold (SAMS) Fabrication…….……...43

3.3.4 Conductivity and Electrochemical Impedance Spectroscopy (EIS)…..... 45

3.3.5 Contact Angle……..…… 45

3.3.6 Actuation Testing……...…..45

3.3.7 C2C12 Cytotoxicity Study …….…….…….……...46

3.3.8 X-ray Photoelectron Spectroscopy (XPS)…….....…….. 47

3.3.9 Statistical Analysis……...47

3.4 Results and Discussion…..……... 47

3.4.1 The effect of Varying GO Concentration in Nanocomposite Hydrophilicity.……...……...47

3.4.2 Electrical Conductivity……... 48

3.4.3 The Effect of Varying the Applied Potential Difference on Angular Movement…… 49

3.4.4 C2C12 Cytotoxicity Study ……...……...49

3.4.5 Discussion……54

3.5 Conclusion ……..……. 57

3.6 References……59

Chapter 1: Background and Introduction

Skeletal muscle is the most abundant tissue in the human body, making up thirty to forty percent of body mass, and is also responsible for any movement by coordinating with the skeleton. Skeletal muscle tissue loss may occur due to several reasons including traumatic injuries, tumor ablation, or infections [1]. One of the most common clinically practiced methods today to treat muscle loss is the use of autologous muscle tissue or muscle flaps from different regions of the skeletal muscle, either local or distant to the area of injury. Despite providing a limited degree of success to return the injured skeletal muscle site to a functioning state, there exists a number of challenges associated with both the donor and the receiver sites. Some of these challenges are the availability of donor sites, tissue design mismatch, donor site morbidity, and loss of functionality leaving patients with major difficulties and diminished quality of life [2].

Human body's natural healing mechanism reserves the power to repair and restore function to small injured sites. However, these mechanisms are often overwhelmed by large volumetric tissue loss as well as formation of scar tissue. Scar tissue formation within skeletal muscle can cause serious limitations in tissue mobility and functionality.

1.1 Skeletal Muscle Anatomy and Physology

Skeletal muscles are made of highly elongated, oriented and multinucleated cells, known as myocytes, developed through the process of myogenesis and fusion of myoblasts. Specialized striated myocytes in the skeletal muscle are known as fibers. Muscle fibers when bound to one another through loose collagenous tissues (perimysium) and supporting tissues (endomysium) result in the formation of bundles called as fascicles [3]. These

muscle fibers vary in length (from a couple of centimeters up to one meter) and diameter (15-100µm) depending on their location and function. For instance, muscles that are responsible for precise and controlled movements are much smaller in size and have more supporting tissue in their surroundings. On the other hand, muscles that are responsible for moving large portions of the human body have much larger fascicles and less supporting tissues. The hierarchical structure of the skeletal muscle along with a cross sectional view of the tissue is shown in *Figure 1*.

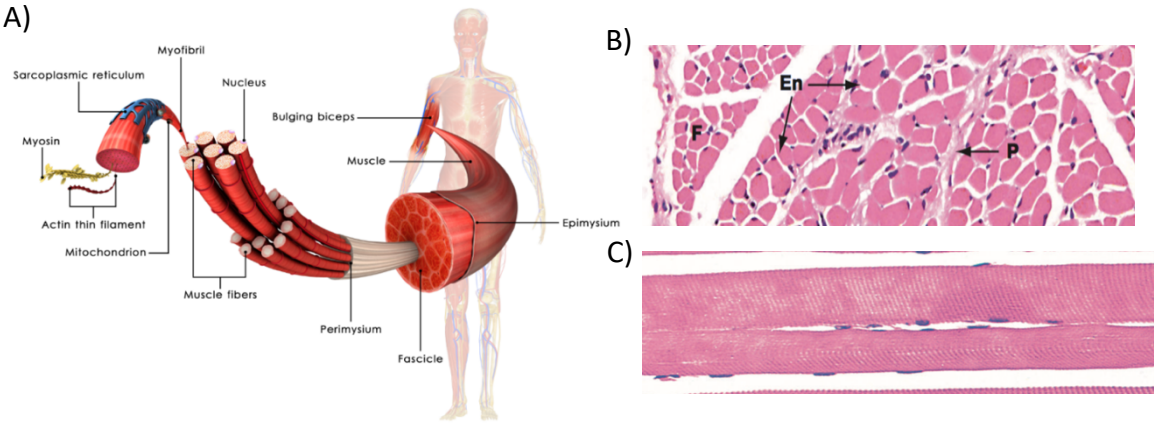

Figure 1 A) Hierarchical Skeletal Muscle structure. Fasicles , blood vessels, and nerve fibers are then wrapped with Epimysium to form a complete muscle tissue. Sarcomeres, which are basic contractile unit of muscles made of contractile proteins such as myosin and actin, are shown. B) cross-sectional image of the muscle tissue depicting the general arrangement of Fascicles (F), Perimysium (P), and endomysium (En). C) Elongated, multinucleated, cylindrical shaped myocytes are shown in the longitudinal section of skeletal muscle. Images are based on a Figure from Young B. and coworkers [3].

Myocytes can be further broken down to myofibrils and sarcomeres. Sarcomeres, known as the basic contractile unit of muscle, are made of contractile myofilaments. A sarcomere contains both thin filaments, made of actin strands, and thick filaments, composed of myosin strands. Sarcomeres are separated via Z-Lines and move closer to one another during a muscle contraction. When muscle is at rest, actin and myosin are inhibited to interact through tropomyosin and troponin blockage of the actin. However, tropomyosin and troponin can release the actin in the presence of calcium ions (Ca^{2+}). Sarcoplasmic

reticulum (SR), a specialized form of endoplasmic reticulum found in muscles, has calcium channels connected to voltage sensing proteins located in the membrane of the muscle cells. When an action potential is sent from the brain through motor neurons, acetylcholine is released at neuromuscular junctions, leading to the activation of sodium channels causing depolarization of the muscle tissue. Action potential is then traveled along the cell membrane and down to the T-Tubules. Consequently, voltage sensitive proteins are stimulated, allowing the passage of calcium ions into the sarcoplasm. Troponin then binds to the available calcium ions and along with tropomyosin are moved away leaving the actin filament exposed for myosin to bind with. Myosin binds with the actin filament through an ATP-dependent cycle that convers ATP to ADP and a phosphate, which then promotes myosin to bind and unbind with the acting filament [4].

For muscle fibers to be able to transfer the created force from their contraction and induce movement to different parts of the body, such as bone or skin, they must be connected to their surrounding connective tissue called the extracellular matrix (ECM). This ECM is made of collagen and elastic fibers that can bear load [5].

In the case of a small and local injury to the skeletal muscle tissue, regeneration occurs when partially differentiated muscle stem cells, also known as satellite cells, travel to the site of the injury and enters into the mitotic stage and further differentiate in response to certain microenvironmental cues, *Figure 2*. Satellite cells then fuse together into organized, elongated, and multinucleated myocytes aimed at connecting the exposed fiber ends. However, for larger defects in which a substantial portion of the skeletal muscle tissue has been destructed and the injured tissue is incapable of regeneration, a different process takes place [2]. In such cases, satellite cells migrate to the site of the injury and in

a process called fibrosis, create a network of connective tissues known as scar tissue, resulting in the loss of functionality of the injured tissue [2]. Both tissue regeneration and scar formation are natural mechanisms involved in wound healing and consist of four interconnected phases of necrosis, inflammation, proliferation, and differentiation of satellite cells [6]. Satellite cell proliferation and differentiation requires a close interaction with neighboring cells and the ECM. In addition, electrochemical, mechanical, and chemical interactions with the microenvironment signal and drive the cells to proliferate and differentiate [5, 7].

Extensive studies on the mechanical properties of skeletal muscles in comparison to scar tissue have shown that connective tissue has much less elasticity than muscle cells. Therefore, scar tissue can limit the functionality and mobility of the muscle tissue. Moreover, skeletal muscle and scar tissue exhibit very different mechanical properties [8,

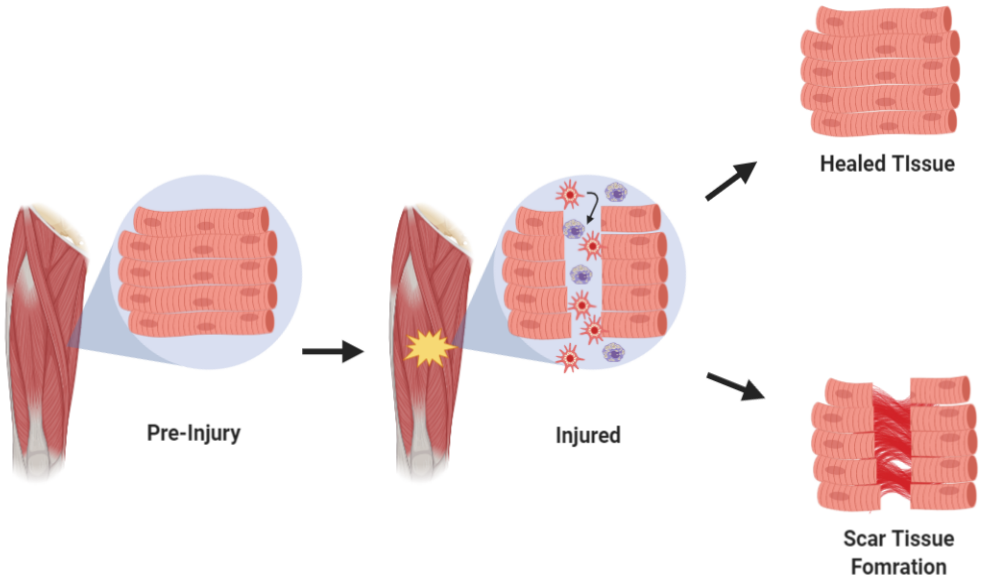

Figure 2 Graphical depiction of the myocyte regeneration or scar tissue formation in a skeletal muscle. The healing process begins soon after injury and the inflammatory response. Satellite cells along with leukocytes rush to the site of the injury. Satellite cells aim to close the gap and fuse the fibers ends to one another. If the muscle loss is larger than a critical size defect, satellite cells differentiate into scar tissue. Scar tissue formation can lead to a significantly reduce tissue's mobility.

9]. For example, scar tissue has a low resistance to rupture with a tendency to be stiffer at lower mechanical loadings and a fast relaxation at lower loads.

1.2 Skeletal Muscle Tissue Engineering

Because of the above listed limitations and challenges associated with muscle flap surgical procedure, current clinical gold standard for volumetric muscle loss treatment, tissue engineering offers great potential alternatives to traditional solutions. The underlying concept of tissue engineering and tissue regeneration has been to recreate a similar process to neoorganogenesis[10]. Although tissue engineers may offer different approaches to promote skeletal muscles regeneration, a general graphical depiction is shown in *Figure 3*. This process usually begins by preforming a biopsy to harvest a population of patients cells having a myogenic potential. These cells are then expanded in-vitro to achieve a suitable

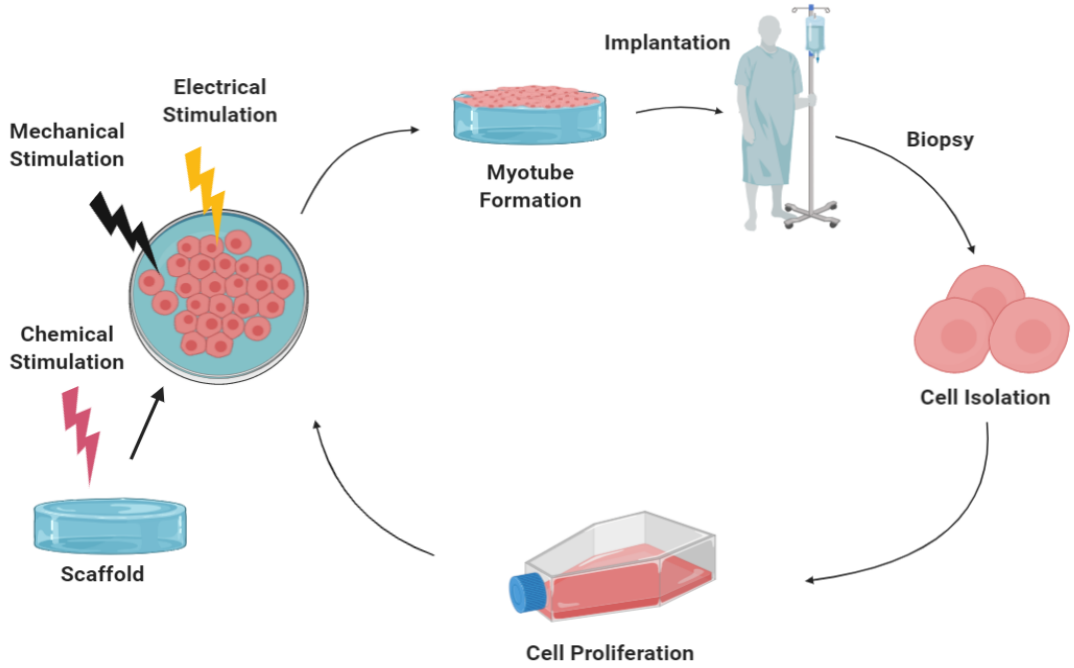

Figure 3 Graphical depiction of tissue engineering. Tissue engineering always begins by extracting patients' primary cells. Cells are then expanded in-vitro conditions and later are placed on a scaffold where they begin the process of differentiation into the target tissue. Cells will be stimulated to mimic the native tissues properties. Cells are then reintroduced and implanted into the patient.

population density. Following expansion, cells are seeded onto a scaffold to provide the necessary three-dimensional microenvironment to achieve differentiation and maturation of cells into myocytes. These scaffolds should be designed to closely match the native tissue's ECM and provide similar mechanical and electrochemical stimulation to the differentiating cells [11-13]. Once cells have completely differentiated into the functional myocytes, they are implanted along with the scaffold into the patient to restore function to the affected location [14, 15].

Scaffold design in tissue engineering is crucial. The scaffold should not only enhance cell attachment, proliferation, and differentiation, but should also be biocompatible and non-immunogenic while promoting seamless integration when implanted with the newly engineered tissue into the host. Since muscle tissue is composed of extremely aligned myocytes, scaffolds used in muscle tissue engineering must promote alignment of cells [16]. Cell alignment can be achieved either by providing topographical guidance, electrical stimulation, or through mechanical guidance [17-19]. Topographical guidance includes the concept of scaffold surface patterning by utilizing techniques such as electrospinning nanofibers and lithography [20, 21]. Cell alignment through electrical stimulation can also be achieved due to the electroactive properties of the muscle cells. Hence, application of an electric field can regulate cell positioning and behavior, further promoting myotube alignment parallel to the electric field [22, 23]. Lastly, myotube alignment thorough mechanical guidance is achieved by cell positioning along the force lines of the scaffold [24]. An engineered skeletal muscle tissue must not only have the ability to respond to electrical stimulation, have large intracellular calcium storage, and acetylcholine receptors, but must also be able to promote self-regeneration after stress-

induced injuries similar to the exercising conditions. Although, so much progress has been made to achieve all the above characterization, to date no tissue engineering scaffold has been developed to promote functional myocytes that meets all of these critical criteria.

It has been previously shown that electrical stimulation of skeletal muscle has significant enhanced formation of myofibers and therefore, improved functional properties of the myocytes[25-27]. Furthermore, electrical stimulation can improve secretion of vascular endothelial growth factors, enhance elongation expression, and improve insulin response by inducing insulin growth factor-1, a myogenic signal molecule, in myocytes [28-30]. Interestingly, long-term electrical stimulation of muscle tissue has led to an increased presence of ECM proteins such as type I collagen and fibrillin [31]. Another study concluded that low voltage electrical stimulation leads to enhanced contractile properties of the C2C12 myocytes [32].

Similarly, mechanical stimulation of engineered tissue has been shown to improve cell development and homeostasis [33]. Thus, such stimulations mimicking *in vivo* physiological conditions can potentially improve scaffold design and lead to engineered tissue's self-repair, maintenance, and regeneration. Previous studies have demonstrated that the type of stress also plays a crucial role in myogenic differentiation. For instance, mechanical stretch of myocytes has led to cytoskeleton remodeling [34]. However, until now, scientists have failed to induce comparable contractile stress on differentiating myocytes, as substrates developed for such purposes can only produce less than one percent contractile stress [35]. Therefore, better tissue engineering scaffold design can improve and promote myogenesis of cells with myogenic potential into fully differentiated,

multinucleated, mature, and capable of exerting contractile stress similar to the native tissue.

1.3 Electroactive polymers and Artificial Muscles for Skeletal Muscle Tissue Engineering

Polymers with the ability to change their size or shape upon being stimulated by an electrical field, are called electroactive polymers (EAP). Also, due to their ability to move repetitively they have been called artificial muscles. Owing to these advantages, EAPs are now being studied in various fields such as robotics, optics, mechatronics, biomedical engineering, fluidics, acoustics, and automation. Similarly, ionic electroactive polymers and electroactive hydrogels take advantage of both free flowing and immobile ions to change size or shape upon electrical stimulation. Herein, we focus on development of electroactive hydrogels and their mechanism of movement. Depending on the hydrogel design, a specific ionic charge, either positive or negative, is fixed to the hydrogel backbone. If a negative charge is fixed inside the hydrogel, then samples are swelled in an ionic solution such as phosphate buffer saline to swell and attract the cations available in the solution. When placed in an active electrical field, cations pull the extremely polar water molecule toward the cathode along with themselves. Therefore, the movement of the hydrogels are linked to the hydrated cations. When a positive charge is fixed to the hydrogel backbone by design, cations in the sample have the ability to move the water molecules toward the negative electrode. Therefore, hydrogels can actuate in either an ionic solution or in pure water, allowing them to be active in a variety of solutions, independent of their ionic composition [36]. However, ionic electroactive hydrogels have their own

shortcomings such as the bending angular motion may not completely mimic the native tissue's contraction, lacks consistent processing and development, and lastly, there have been issues identified to upscale the current designs [37].

Ionic electroactive polymers have been shown to provide a contractile force similar to muscle tissue at a range of 0.1-40MPa [37]. Therefore, modification of these hydrogels could potentially improve tissue engineering scaffold design. Also, both electroactive hydrogel and the skeletal muscle tissue are prompted to move on a similar ionic basis. As previously stated, skeletal muscle movement starts with the ionic depolarization of the muscle membrane that further leads to the release of calcium ions into the sarcoplasm. Similarly, ionic electroactive hydrogels are actuated through the interaction of backbone charges and the free-flowing ions. As depicted in *Figure 4*, through polymerization and further modification of electroactive hydrogels, it may be possible to design 3D cell scaffold that can provide the necessary mechanical and electrical stimulation and improve myocyte differentiation and maturation.

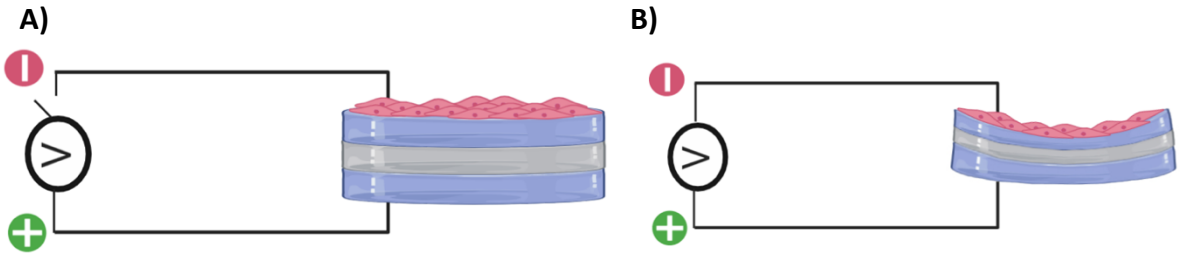

Figure 4 Graphical depiction of electroactive hydrogel used in tissue engineering scaffold design. Copolymerization permitting a superior design for skeletal muscle scaffolds, because they have the ability to interact with the cells through electrical and mechanical stimuli. Outer layers are made of conductive material that would act as the electrodes. And external power source will apply the potential difference to not only stimulate cells but at the same time actuate the hydrogels, which would in turn mechanical stimulate the cells. A) system at rest with no potential difference applied, B) Circuit is complete and there is a potential difference, which leads to ion manipulation and actuation of the hydrogels as the result.

The central objective of this project is to develop a scaffold that could mimic the native tissues movement and electrochemical composition while enhancing myoblast adhesion, proliferation, and differentiation into highly functional myocytes. To that end, successful completion of this project will advance the skeletal muscle tissue engineering field as this novel and active scaffolds are not only capable of electrically and mechanically stimulating cells *in vitro*, but upon *in vivo* implantation at the injured site, can temporarily generate comparable force until the developing tissue fuses to the damaged myocyte endings.

1.4 Project Goal and Specific Aims

The goal of this project is to develop, optimize, and characterize actuating EAP to be used as stimulating and interactive skeletal muscle scaffolds for tissue engineering purposes. To achieve this, the following specific aims will be studied:

Specific Aim 1: To develop, characterize and optimize positively charged Poly(Ethylene Glycol) Diacrylate based hydrogels as skeletal muscle tissue engineering scaffold. We hypothesize that a positively charged EAP can demonstrate enhanced bending motion while improving cellular attachment, proliferation, and differentiation thus, acting as a skeletal muscle scaffold. We will examine this hypothesis by developing a hydrogel scaffold using Poly(Ethylene Glycol) Diacrylate copolymerized with 2-(methacryloyloxy) ethyl trimethylammonium chloride (MAETAC).

Specific Aim 2: To develop, optimize, and evaluate a biocompatible and highly electroconductive self-actuating multilayer hydrogel as skeletal muscle tissue

engineering scaffold. We hypothesize that a biocompatible multilayer hydrogel constructed with highly electroconductive, positively, and negatively charged layers can demonstrate enhanced bending motion and reduced applied voltage. To examine this hypothesis, we will develop a multilayer electroactive scaffold with poly(ethylene glycol) diacrylate (PEGDA) hydrogel copolymerized with poly(3,4 ethylenedioxythiophene):polystyrenesulfonate (PEDOT:PSS), 2-(methacryloyloxy) ethyl-trimethylammonium chloride, and acrylic acid monomer (AA).

References

1. Baghdadi, M.B. and S. Tajbakhsh, *Regulation and phylogeny of skeletal muscle regeneration.* Developmental Biology, 2018. **433**(2): p. 200-209.
2. Bach, A.D., et al., *Skeletal muscle tissue engineering.* Journal of Cellular and Molecular Medicine, 2004. **8**(4): p. 413-422.
3. Young, B., *Wheater's Functional Histology A Text and Colour Atlas*. 6th ed. 2000: Fourth edition / by Barbara Young, John W. Heath ; with contributions by Alan Stevens, James S. Lowe ; drawings by Philip J. Deakin. Edinburgh ; New York : Churchill Livingstone, 2000.
4. Marieb, E.N., *Essentials of human anatomy & physiology*. 1991: Third edition. Redwood City, Calif. : Benjamin/Cummings Pub. Co., [1991] ©1991.
5. Gillies, A.R. and R.L. Lieber, *STRUCTURE AND FUNCTION OF THE SKELETAL MUSCLE EXTRACELLULAR MATRIX.* Muscle & Nerve, 2011. **44**(3): p. 318-331.
6. Barberi, L., et al., *Age-dependent alteration in muscle regeneration: the critical role of tissue niche.* Biogerontology, 2013. **14**(3): p. 273-292.
7. Valentin, J.E., et al., *Functional skeletal muscle formation with a biologic scaffold.* Biomaterials, 2010. **31**(29): p. 7475-7484.
8. Corr, D.T. and D.A. Hart, *Biomechanics of Scar Tissue and Uninjured Skin.* Advances in Wound Care, 2013. **2**(2): p. 37-43.
9. Shah RG, S.F., *Vibrational analysis of extracellular matrix scaffolds: comparison of skin, dermis, cartilage and subchondral bone using oct and vibrational analysis.* Adv Tissue Eng Regen Med Open Access, 2017.
10. Mooney DJ, M.A., *Growing new organs.* Sci Am., 1999
11. Machingal, M.A., et al., *A Tissue-Engineered Muscle Repair Construct for Functional Restoration of an Irrecoverable Muscle Injury in a Murine Model.* Tissue Engineering Part A, 2011. **17**(17-18): p. 2291-2303.
12. Corona, B.T., et al., *Implantation of In Vitro Tissue Engineered Muscle Repair Constructs and Bladder Acellular Matrices Partially Restore In Vivo Skeletal Muscle Function in a Rat Model of Volumetric Muscle Loss Injury.* Tissue Engineering Part A, 2014. **20**(3-4): p. 705-715.

13. Huang, Y.C., et al., *Rapid formation of functional muscle in vitro using fibrin gels.* Journal of Applied Physiology, 2005. **98**(2): p. 706-713.
14. Seidi, A., et al., *Gradient biomaterials for soft-to-hard interface tissue engineering.* Acta Biomaterialia, 2011. **7**(4): p. 1441-1451.
15. VanDusen, K.W., et al., *Engineered Skeletal Muscle Units for Repair of Volumetric Muscle Loss in the Tibialis Anterior Muscle of a Rat.* Tissue Engineering Part A, 2014. **20**(21-22): p. 2920-2930.
16. Browe, D. and J. Freeman, *Optimizing C2C12 myoblast differentiation using polycaprolactone-polypyrrole copolymer scaffolds.* Journal of Biomedical Materials Research Part A, 2019. **107**(1): p. 220-231.
17. Nikkhah, M., et al., *Engineering microscale topographies to control the cell-substrate interface.* Biomaterials, 2012. **33**(21): p. 5230-5246.
18. Curtis, A. and C. Wilkinson, *Topographical control of cells.* Biomaterials, 1997. **18**(24): p. 1573-1583.
19. Pennisi, C.P., et al., *Uniaxial Cyclic Strain Drives Assembly and Differentiation of Skeletal Myocytes.* Tissue Engineering Part A, 2011. **17**(19-20): p. 2543-2550.
20. Xia, Y. and G.M. Whitesides, *Soft Lithography.* Angewandte Chemie International Edition, 1998. **37**(5): p. 550-575.
21. Higuchi, A., et al., *Physical Cues of Biomaterials Guide Stem Cell Differentiation Fate.* Chemical Reviews, 2013. **113**(5): p. 3297-3328.
22. Hosseini, V., et al., *Engineered Contractile Skeletal Muscle Tissue on a Microgrooved Methacrylated Gelatin Substrate.* Tissue Engineering Part A, 2012. **18**(23-24): p. 2453-2465.
23. Ahadian, S., et al., *Interdigitated array of Pt electrodes for electrical stimulation and engineering of aligned muscle tissue.* Lab on a Chip, 2012. **12**(18): p. 3491-3503.
24. Akiyama, Y., et al., *Rod-shaped Tissue Engineered Skeletal Muscle with Artificial Anchors to Utilize as a Bio-Actuator.* 2010.
25. Brevet, A., et al., *MYOSIN SYNTHESIS INCREASED BY ELECTRICAL-STIMULATION OF SKELETAL-MUSCLE CELL-CULTURES.* Science, 1976. **193**(4258): p. 1152-1154.
26. Pette, D. and G. Vrbova, *What does chronic electrical stimulation teach us about muscle plasticity?* Muscle & Nerve, 1999. **22**(6): p. 666-677.
27. De Deyne, P.G., *Formation of sarcomeres in developing myotubes: role of mechanical stretch and contractile activation.* American Journal of Physiology-Cell Physiology, 2000. **279**(6): p. C1801-C1811.
28. Kanno, S., et al., *Establishment of a simple and practical procedure applicable to therapeutic angiogenesis.* Circulation, 1999. **99**(20): p. 2682-2687.
29. Brutsaert, T.D., et al., *Regional differences in expression of VEGF mRNA in rat gastrocnemius following 1 hr exercise or electrical stimulation.* BMC physiology, 2002. **2**: p. 8-8.
30. Aas, V., et al., *Electrical stimulation improves insulin responses in a human skeletal muscle cell model of hyperglycemia*, in *Lipids and Insulin Resistance: The Role of Fatty Acid Metabolism and Fuel Partitioning*, I. Klimes, et al., Editors. 2002. p. 506-515.

31. Trumble, D.R., et al., *The Effects of Long-Term Stimulation on Skeletal Muscle Phenotype Expression and Collagen / Fibrillin Distribution.* 2002.
32. Thelen, M.H.M., W.S. Simonides, and C. vanHardeveld, *Electrical stimulation of C2C12 myotubes induces contractions and represses thyroid-hormone-dependent transcription of the fast-type sarcoplasmic-reticulum Ca2+-ATPase gene.* Biochemical Journal, 1997. **321**: p. 845-848.
33. Bansai, S., et al., *Effect of Cyclic Stretch on Tissue Maturation in Myoblast-Laden Hydrogel Fibers.* Micromachines, 2019. **10**(6).
34. Hornberger, T.A., et al., *Intracellular signaling specificity in response to uniaxial vs. multiaxial stretch: implications for mechanotransduction.* American Journal of Physiology-Cell Physiology, 2005. **288**(1): p. C185-C194.
35. Kosnik, P.E., J.A. Faulkner, and R.G. Dennis, *Functional development of engineered skeletal muscle from adult and neonatal rats.* Tissue Engineering, 2001. **7**(5): p. 573-584.
36. Scott, T.E., et al., *Characterization and optimization of a positively charged poly (ethylene glycol)diacrylate hydrogel as an actuating muscle tissue engineering scaffold.* Polymers for Advanced Technologies.
37. Bar-Cohen, Y., *Electroactive Polymer (EAP) Actuators as Artificial Muscles: Reality, Potential, and Chaleneges.* The International Society for Optical Engineering, 2004.

Chapter 2: Characterization and Optimization of a Positively Charged Poly(Ethylene Glycol) Diacrylate Hydrogel as an Actuating Muscle Tissue Engineering Scaffold

(Published Manuscript, July of 2019)

2.1 Abstract

Hydrogels have been used for many applications in tissue engineering and regenerative medicine due to their versatile material properties and similarities to the native extracellular matrix. Poly(ethylene glycol) diacrylate (PEGDA) is an ionic electroactive polymer (EAP), a material that responds to an electric field with a change in size or shape while in an ionic solution, that may be used in the development of hydrogels. In this study we have investigated a positively charged EAP that can bend without the need of external ions. PEGDA was modified with the positively charged molecule 2-(methacryloyloxy) ethyl-trimethylammonium chloride (MAETAC) to provide its own positive ions. This hydrogel was then characterized and optimized for bending and cellular biocompatibility with C2C12 mouse myoblast cells. Studies show that the polymer responds to an electric field and supports C1C12 viability.

2.2 Introduction

Hydrogels have been used extensively in tissue engineering and regenerative medicine due to their structural and compositional similarity to the native extracellular matrix [1]. Their material properties are tunable based on their method of design. Some can be used as an injectable for tissue repair, be photopolymerized into various shapes, are biodegradable, nontoxic, and nonimmunogenic.

Poly(ethylene glycol) (PEG) also known as poly(ethylene oxide) or poly(oxyethylene) has been one of the most widely explored polymers in biomedicine. In

addition to the hydrogel properties mentioned above, PEG is a hydrophilic polymer that can be modified through grafting and copolymerization to increase its biodegradability [2-5]. Unfortunately, PEG based hydrogels have a lower cell attachment rate due to the formation of a hydrated surface layer that inhibits the adsorption of adhesion specific proteins such as fibronectin. In spite of this studies have shown that altering these hydrogels with various additional components can enhance cell attachment [6-10].

An electroactive polymer (EAP) is a polymer that responds with a change in size or shape after being introduced to an electric field. Ionic electroactive polymers are EAPs that swell in an ionic solution. Upon electrical stimulation the ions in solution are attracted to the oppositely charged electrode and will pull accompanying water molecules with them causing one side of the polymer to swell and produce a bending motion. Specifically, when a negatively charged EAP is placed into an ionic solution it attracts positive ions (cations) that are bound to water (a polar molecule). When an electric field is produced these cations move toward the negative electrode, bringing the water with them. This causes one side of the polymer to swell and the other side to shrink, producing a bending motion. A majority of the investigated EAP are negatively charged and bend by this mechanism, so they can only actuate in an ionic solution. Since the movement of water is linked to the presence of positive cations in the solution a polymer that is positively charged may be more versatile. The presence of cations that are already bound to the polymer should allow it to actuate in either an ionic solution or in pure water, allowing it to be active in a variety of solutions, including biological solutions.

To test this theory, we chose to modify poly(ethylene glycol) diacrylate (PEGDA) with the positively charged molecule 2-(methacryloyloxy) ethyl-trimethylammonium

chloride (MAETAC). This material has been used in other studies with osteoblasts to improve cell attachment. It is believed that the cationic charges within MAETAC lead to enhanced absorption of the anionic extracellular matrix (EMC) proteins [11]. As stated earlier, the positive charge associated with MAETAC could also provide the added benefit of inherently containing positive ions within the hydrogel that can be attracted to the negative electrode and thus pull the water within the hydrogel to one side causing it to swell, allowing it to bend in that direction without the need of ions from the surrounding environment. In this study we explore the effects of a positive charge on myoblast attachment and determine if the presence of positive charges enhance the actuation properties of our self-actuating hydrogel in saline and pure water, for potential use in muscle tissue engineering.

2.3 Methods and Materials

2.3.1 Hydrogel preparation and swelling

PEGDA of molecular weights 1000 Da, 4000 Da, 8000 Da, and 10,000 Da were purchased from Monomer-Polymer and Dajac Labs (an MPD Chemicals Company). MAETAC, 2,2-Dimethoxy-2-phenylacetophenone, and 1-Vinyl-2-pyrrolidinone was purchased from Sigma Aldrich. The photo-initiator solution of 300 mg/mL of 2,2-Dimethoxy-2-phenylacetophenone in 1-Vinyl-2-pyrrolidinone was prepared using a vortex mixer.

The hydrogels were formed by dissolving the PEGDA into DI water using a vortex mixer. The MAETAC was then added and vortexed until sufficiently mixed. Various formulations were created to obtain a hydrogel with the best blend of actuation and biocompatibility. The formulations for each of the samples are listed in Table 1. The photo-

initiator solution was added just prior to applying UV radiation at a concentration of 100 µL of photo-initiator solution per 1 mL of hydrogel solution. The hydrogel solution was then injected into a rectangular glass mold and crosslinked with UV radiation at a wavelength of 365 nm and intensity of 10W for 2 minutes. The hydrogels were then placed in phosphate buffered solution (PBS) overnight to achieve equilibrium swelling. For actuation testing samples were cut into 20 mm x 5 mm shapes before actuation.

Table 1: Formulations and geometry of the various hydrogel samples. The name of the hydrogel sample emphasizes the change in formulation or geometry of each sample. The values that are bold indicate the values that have been changed.

Name of Hydrogel sample	Molecular weight of PEGDA(Da)	Amount of MAETAC(µl)	Amount of PEGDA(g)	Amount of Water(ml)	Concentration of PEGDA(g/ml)	Thickness to length ratios
1000	1000	60	0.1	1	0.1	0.0275
4000	4000	60	0.1	1	0.1	0.0275
8000	8000	60	0.1	1	0.1	0.0275
10000	10000	60	0.1	1	0.1	0.0275
40	8000	40	0.1	1	0.1	0.0275
60	8000	60	0.1	1	0.1	0.0275
80	8000	80	0.1	1	0.1	0.0275
120	8000	120	0.1	1	0.1	0.0275
150	8000	150	0.1	1	0.1	0.0275
160	8000	160	0.1	1	0.1	0.0275
0.1	8000	60	0.1	1	0.1	0.0275
0.1334	8000	60	0.1	0.75	0.1334	0.0275
0.2	8000	60	0.1	0.5	0.2	0.0275
0.0275	8000	60	0.1	1	0.1	0.0275
0.042	8000	60	0.1	1	0.1	0.042
0.0485	8000	60	0.1	1	0.1	0.0485
HS-1	8000	60	0.1	1	0.1	0.0275
HS-2	8000	60	0.1	0.75	0.1334	0.0275
HS-3	8000	40	0.1	1	0.1	0.0275
HS-4	8000	40	0.1	0.75	0.1334	0.0275

2.3.2 FTIR spectroscopy

Fourier Transform Infrared (FTIR) spectroscopy was performed to characterize the hydrogels and verify the presence of the methacroyl carbonyl from the MAETAC. The samples were lyophilized before being placed in a Thermo Scientific Nicolet iS10 FTIR spectrometer and the background (air) readings were subtracted out.

2.3.3 Actuation tests

All hydrogel specimens were cut into 20 mm x 5 mm samples and stored in PBS until the time of testing. In Table 1, samples with a thickness to length ratio of 0.0275 had a thickness of 0.55 mm, samples with a thickness to length ratio of 0.042 had a thickness of 0.84 mm, samples with a thickness to length ratio of 0.0485 had a thickness of 0.97 mm. All testing was done in triplicate, n = 3, on a testing device previously used in a similar study [6]. Briefly, the sample was placed in the actuation device (*Figure 1*) which consisted of a small petri dish with two small pegs affixed at the center to hold the sample in place. Two platinum electrodes were also affixed to the device 3.0 cm apart with the sample centered in between them. The electrodes were constructed from four 99.5% pure platinum wires of 0.20mm diameter twisted together. The actuation device was filled with PBS. An Agilent Dual Output DC Power Supply (E3646A Agilent Technologies, Santa Clara, CA, USA) was used to provide 20 V for a maximum of 5 minutes. All actuation tests were recorded using the video mode of a digital camera. The video was then analyzed to determine angular movement.

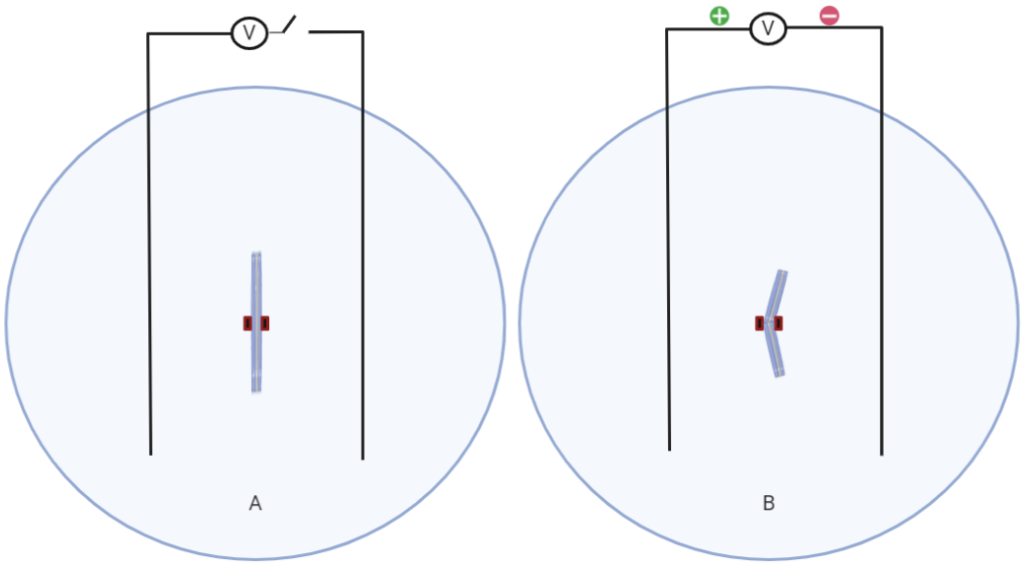

Figure 1: Schematic of the device used for actuation testing of the hydrogel samples. A) Prior to application of 20 Volts. B) Upon electrical stimulation, the hydrogel bends due to the movement of ions and accompanying water.

2.3.4 Effect of Solution Ions on Actuation

Typically, electroactive ionic polymers actuate through the movement of solvent ions. The negative charges in the polymer attract the positive cations in the solution. These cations are bound to water, moving more water into the polymer and closer to the negatively charged electrode. The electroactive ionic polymer in this study is positively charged. Theoretically the water would be attracted to the cations in the electroactive ionic polymer. The cations in the polymer would move toward the negatively charged electrode, moving the water with them. This would allow the hydrogel to move in pure water and an ionic solution; the cations may be hindered through their linkages to the polymer backbone, which may hinder the degree of polymer actuation.

In order to evaluate the effect of pure water on hydrogel actuation PEG with molecular weights of 1000 and 8000 were crosslinked with various amounts of MAETAC (40, 60,

80, and160µl). These samples were then subjected to the same actuation experiments described earlier, except deionized water was used instead of PBS.

2.3.5 Contractile Strength

All hydrogel specimens were again cut into 20 mm x 5 mm samples (with the mentioned thickness in Table 1) and tested in triplicate, n = 3. The sample was suspended in PBS in a vertical bath between two platinum electrodes. The electrodes consisted of four platinum wires twisted together (each wire was 99.5% pure and 0.20mm diameter). Each electrode was then bent into a sinusoidal waveform to cover more area. Aluminum foil weights of increasing value were placed on the free end of the hydrogel. Again, a DC voltage of 20 V from the Agilent Dual Output DC Power Supply was used for a maximum of 5 minutes to obtain movement from the hydrogel. If the hydrogel was able to produce enough force to lift the aluminum foil weight, the contractile stress was calculated, taking into account buoyancy. Using the equation below where $\sigma_{Contraction}$ is the contractile stress produced by the hydrogel, m_H is the mass of hydrogel, m_{Al} is the mass of the aluminum weight, V_H is the volume of hydrogel, V_{Al} is the volume of aluminum, ρ_{H_2O} is the density of water, and g is the acceleration due to gravity, and A_H is the cross sectional area of the hydrogel.

$$\sigma_{Contraction} = \frac{\left[(m_H + m_{Al}) - (V_H + V_{Al})\rho_{H_2O}\right]g}{A_H}$$

2.3.6 Polymer Biocompatibility

Hydrogel samples, n = 4, were cut into circles with a 15mm diameter to fit into 24-well culture plates. The samples were sterilized by rinsing briefly in ethanol and exposing to UV light for 30 min on each side. The samples were then washed in sterile PBS and soaked overnight in DMEM media containing 10% fetal bovine serum (FBS) and 1% penicillin/streptomycin (P/S). Every well was seeded with approximately 60,000 C2C12 mouse myoblast cells (30,000 cells/cm^2), which were purchased from the American type culture collection (ATCC).

Biocompatibility, metabolic activity and cellular proliferation were assessed at 1, 3, and 7 days after cell seeding using a PrestoBlue® cell viability assay. At each time point the media from all wells were removed and replaced with the PrestoBlue® reagent diluted with media at a ratio of 1:10. After an incubation period of one hour, the absorbance was read on a Tecan Infinite M200 PRO plate reader at 570 nm. Cell morphology was also examined at days 1, 3, and 7 by fixing the cells with a 3.7% paraformaldehyde solution and staining the cells with NucBlue® fixed cell ReadyProbes® reagent (Thermo Fisher Scientific) for DNA and Fluorescein Phalloidin (Thermo Fisher Scientific) for F-actin.

2.3.7 Statistics

All data was presented in the form of average and standard deviation. The data was evaluated with a one-way analysis of variance (ANOVA) with a Tukey's post-hoc test to determine the statistical significance. The significance was set at $p < 0.05$.

2.4 Results

2.4.1 FTIR spectroscopy

The FTIR spectra are shown in *Figure 2* for a PEGDA sample and two samples of the PEGDA-MAETAC hydrogel containing two amounts of MAETAC (40 µL and 120 µL). The copolymerization of the PEGDA and MAETAC produced a new peak at 1725 cm^{-1}. This peak represents the methacroyl carbonyl from the MAETAC. The intensity of the peak also increased with increasing concentrations of MAETAC.

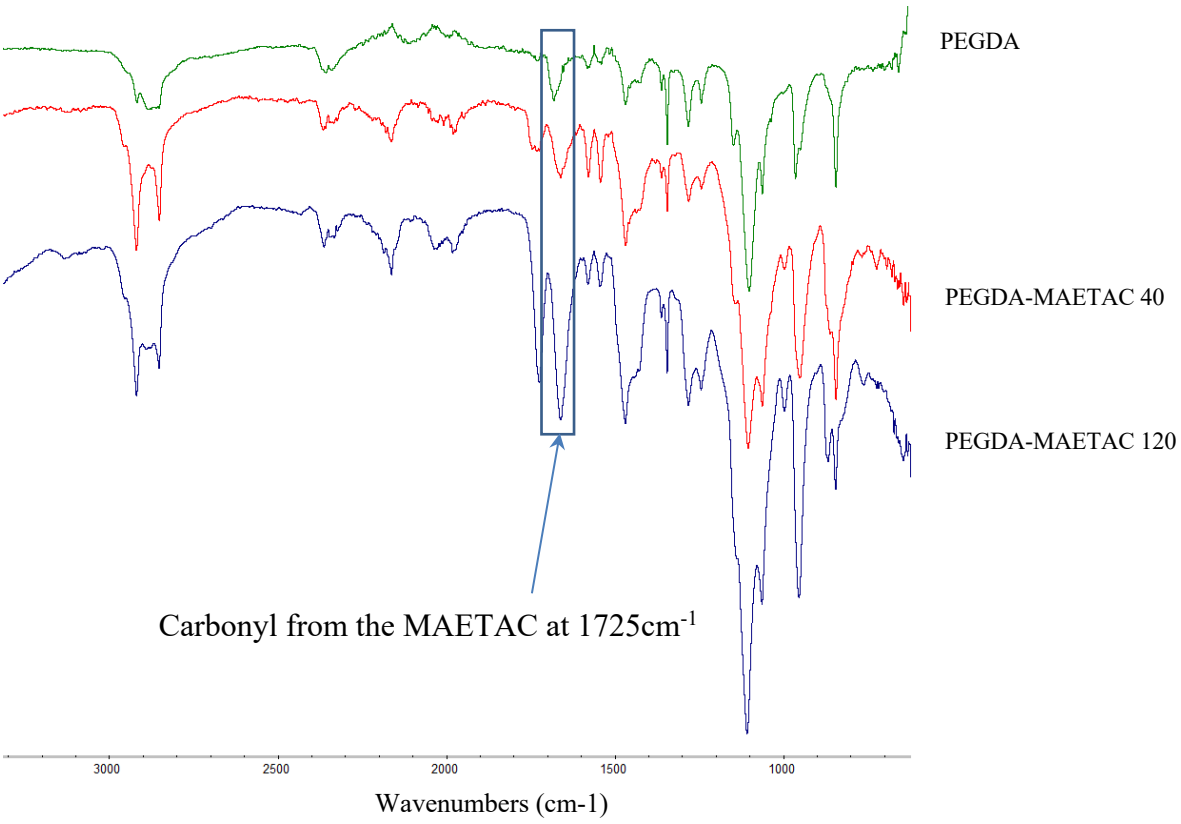

Figure 2: FTIR spectra of PEGDA and two concentrations of PEGDA-MAETAC hydrogels.

2.4.2 The Effects of Varying the Molecular Weight of PEGDA

To determine the optimal formulation of the PEGDA/ MAETAC hydrogel, numerous actuation tests were performed with four different of molecular weights of PEGDA (1000 Da, 4000 Da, 8000 Da, and 10,000 Da), Table 1. The amount of movement produced by the hydrogel when stimulated in PBS is shown in *Figure 3*. Although there appears to be a downward trend with increasing molecular weights of PEGDA, from 52.5° for the 1000 Da PEGDA to 24. 27° for the 10,000 Da PEGDA, only the difference between the 1000 Da samples and the 10,000 Da samples were statistically significant.

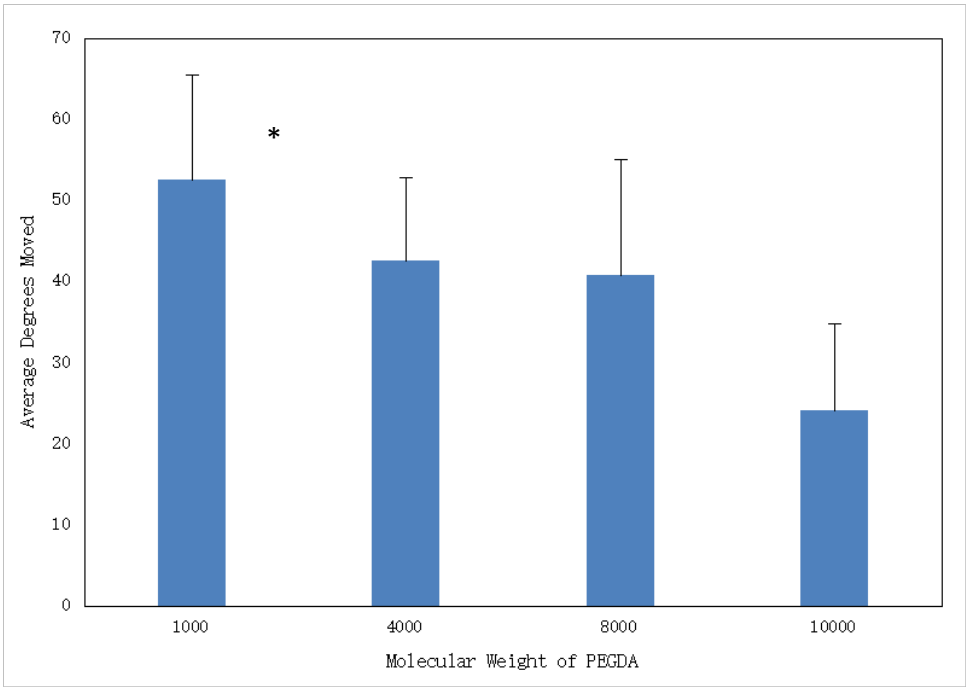

Figure 3: The effects of varying the molecular weight of PEGDA on the amount of bending produced by the hydrogel as measured in degrees. The * indicates a statistically significant increase over 10,000 MW PEGDA (P< 0.05). PEGDA 4000 Da, PEGDA 8000 Da, and PEGDA 10,000 Da actuation results were not significantly different when analyzed using one-way ANOVA and a post hoc tukey test. As seen the lower molecular weight of PEGDA actuated to a higher degree in comparison with the PEGDA with a higher molecular weight.

2.4.3 The Effects of Varying the Concentrations of MAETAC and PEGDA

The amount of MAETAC in the formulation was varied to determine its effect on the amount of bending achieved by the hydrogel. Five different amounts of MAETAC were

tested 40 µL, 60 µL, 80 µL, 120 µL, and 160 µL, Table 1. As the amount of MAETAC increased so did the amount of time needed to crosslink the hydrogel. The time was increased in increments of 30 seconds, from 1 minute and 30 seconds for the 40 µL hydrogel to 2 minutes and 30 seconds for the 160 µL hydrogel. Unfortunately, as the amount of MAETAC was increased, the integrity of the hydrogel began to decrease. Even though the 120 µL hydrogels displayed the largest amount of actuation, it was not an ideal choice due to difficulty in handling the hydrogel. Along with the reduced integrity, the hydrogel that contained 160 µL of MAETAC did not actuate at all during testing, therefore it was not included in *Figure 4*.

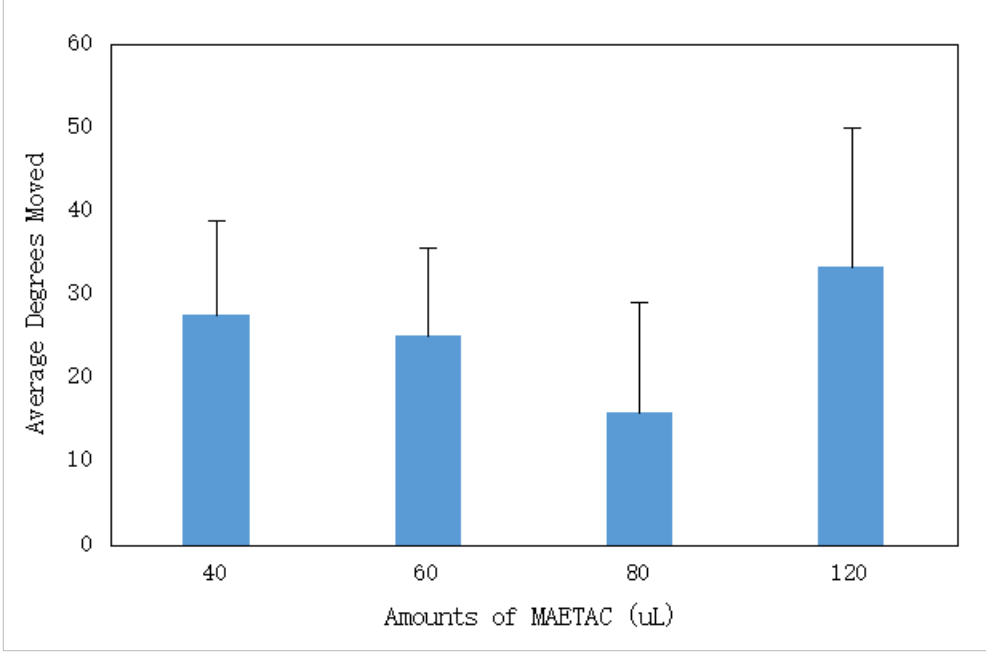

Figure 4: The effects of varying the amount of MAETAC on the amount of bending produced by the hydrogel in PBS as measured in degrees. There was no statistically significant difference between the groups. The integrity of hydrogels began to decrease as the amount of the added MAETAC increased.

Various amounts of MAETAC were used in creation of the hydrogels to test their angular movements in deionized water. As previously mentioned, the integrity of hydrogels decreased as the amount of added MAETAC increased. Therefore, the crosslinking time

was increased by 60 seconds from 2 minutes to 3 minutes for the 80 µL and 160 µL hydrogel samples. A One-way ANOVA and post hoc Tukey test was used to analyze the statistical differences between samples, a p value ≤0.05 was considered statistically significant. Differences in degrees of movement between hydrogel samples of 40 µL, 60 µL, and 80 µL were statistically insignificant. On the contrary, the 160 µL hydrogel sample had a p value <0.05 in comparison with every other sample group. Actuation results of these hydrogels can be seen in *Figure 5*. We also compared the actuation results of the varying amounts of MAETAC with PEGDA-8000 Da with those of PEGDA-1000 Da and the results are shown in *Figure 6*.

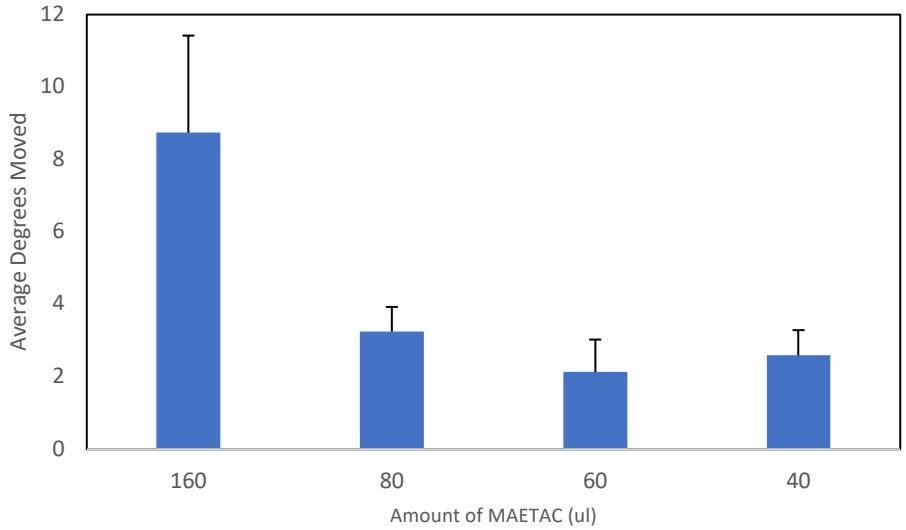

Figure 5: The effects of varying the amount of MAETAC on the amount of bending produced by the hydrogel in deionized water with PEGDA-8000, as measured in degrees. A One-way ANOVA and post hoc Tukey test showed that differences in degrees of movement between hydrogel samples of 40 µL, 60 µL, and 80 µL were statistically insignificant (P>0.05). However, the samples wit 160 µL showed a statistical significance when compared with other groups (P<0.05).

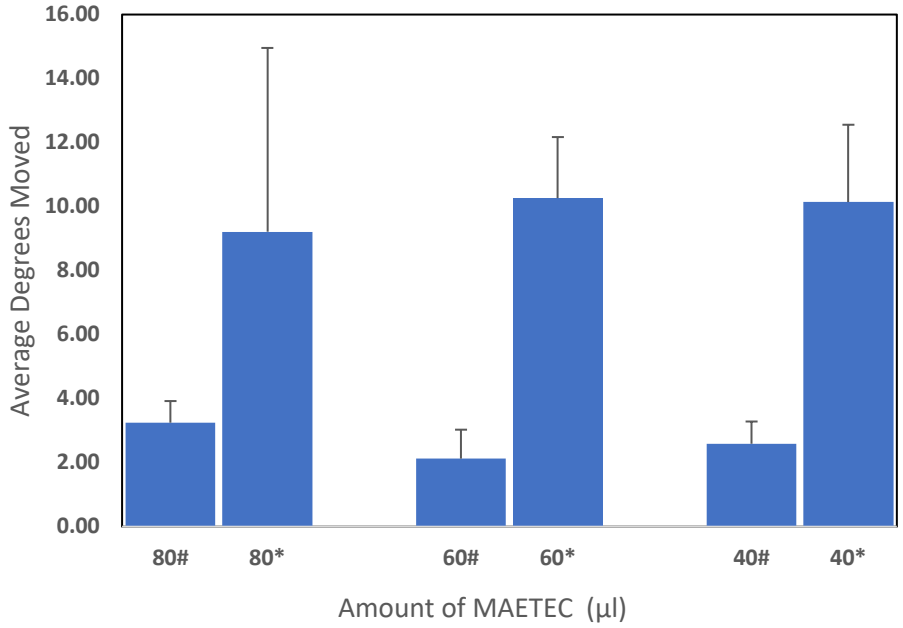

Figure 6: The effects of varying the amount of MAETAC on the amount of bending produced by the hydrogel in deionized water with PEGDA-8000 versus PEGDA-1000, as measured in degrees. * Represent data related to PEGDA-1000 Da, and # represents data related to PEGDA-8000 Da. Both # and * groups in 60 and 40 µl showed a significant difference with a p value <0.05.

The total concentration of the copolymer PEGDA:MAETAC was also varied by altering the amount of DI water used during crosslinking. The concentration of PEGDA in the formulation was increased from 0.1 g/ml to 0.1334 g/ml and then to 0.2 g/ml. The change in concentration did not have a significant effect on the actuation of the hydrogel as can be seen in *Figure 7*.

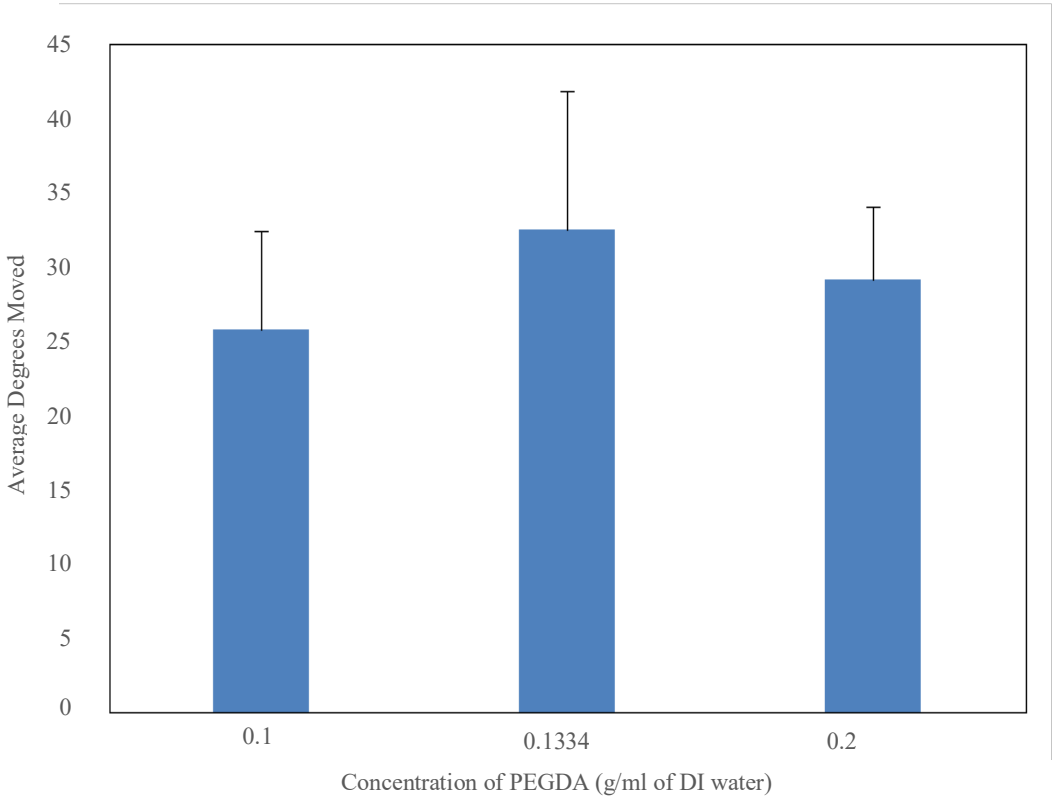

Figure 7: The effects of varying the concentration of PEGDA on the amount of bending produced by the hydrogel as measured in degrees. Varying concentration of PEGDA from 0.1g.mL to 0.2 g/mL did not cause a significant difference in the movement of the hydrogels in the electrical field.

2.4.4 The Effects of Varying Hydrogel Thickness

The thickness of the hydrogel was varied to determine if there was an optimal thickness to length ratio for actuation. The lengths of all the samples were 20 mm. The thickness to length ratios used were 0.0275, 0.042 and 0.0485 as shown in *Figure 8*. The ratio of 0.0275 significantly larger than the other two values.

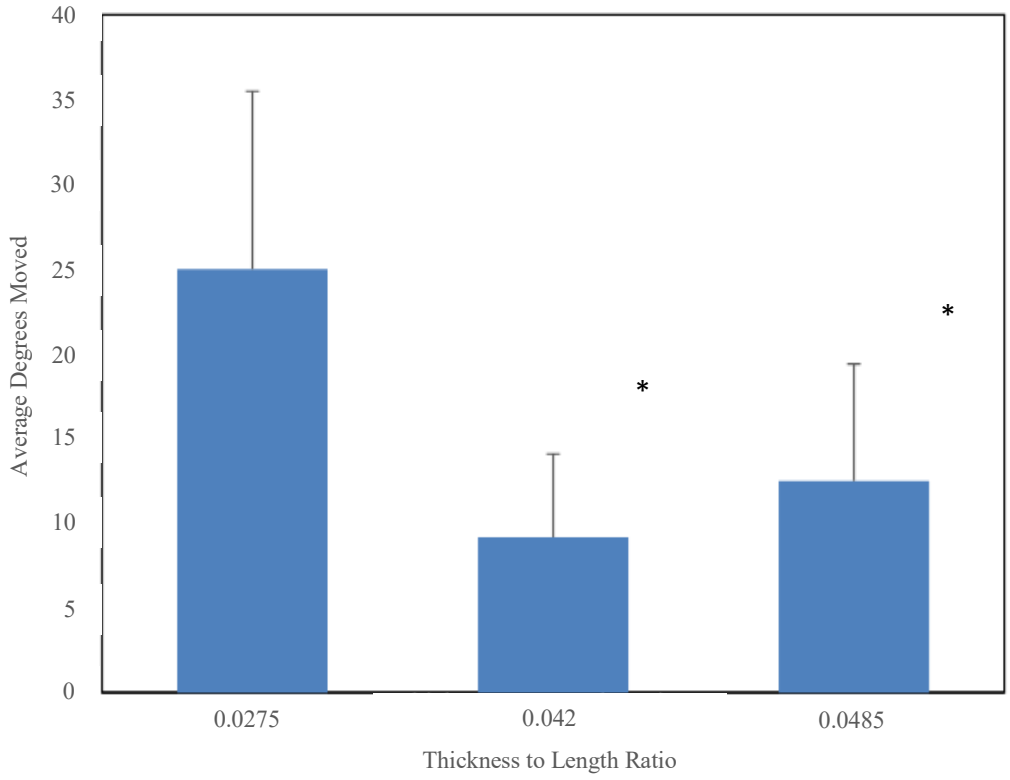

Figure 8: The effects of varying the thickness to length ratios of the hydrogel on the amount of bending produced by the hydrogel as measured in degrees (* P< 0.05, compared to the 0.0275 ratio). This indicates that movement of tested hydrogels increased as their thickness reduced.

2.4.5 Contractile Strength

Based on the findings of the previous actuation tests, four hydrogel formulations were tested for contractile strength. The four formulations contained varying amounts of polymer concentrations as shown in Table 1, HS-1 thru HS-4. The values obtained for the contractile stresses produced are shown in Table 2 and ranged from 120.21 Pa to 153.72 Pa. Although the stress produced by sample 1 was the largest, there were no significant differences in the stresses produced by all the hydrogel samples.

Table 2: Stress produced by each hydrogel (n=3). HS-1 and HS-3 are representing 60µl and 40 µl of MAETAC with 0.1 g/ml of PEGDA in DI water. HS-2 and HS-4 are representing samples with 60µl and 40 µl of MAETAC with 0.1334 g/ml of PEGDA in DI water. Based on these results, increasing PEGDA concentration reduces the average produced force, but increasing the amount of MAETAC in samples leads to an increase in force production.

Hydrogel sample	Average Stress Produced by Hydrogel (Pa)
HS-1	153.72±21.41
HS-2	120.21±14.81
HS-3	129.05±14.82
HS-4	127.92±20.35

2.4.6 C2C12 Cytotoxicity Study

In this study, C2C12 cells were seeded on the same four types of hydrogels used in the contractile strength measurements. Cells were also seeded on a PEGDA hydrogel that did not contain MAETAC and tissue culture polystyrene (TCP) as a positive control. The metabolic activity of the cells is shown for days 1, 3, and 7 in *Figure 9*. As was expected the cells on TCP yielded the highest levels of metabolic activity while the PEGDA had the least. There were no significant differences between any of the groups of PEGDA-MAETAC either comparing the four different samples within each timepoint or comparing the same hydrogel sample across the three different timepoints.

The cells were stained with NucBlue® fixed cell ReadyProbes® reagent (DAPI) for DNA and Fluorescein Phalloidin for F-actin on days 1, 3 and 7 in order to assess cellular attachment and morphology, as shown in *Figure 10*. Cell proliferation was consistent for all samples with the exception of the PEGDA hydrogel. As can be seen in *Figure 8K & L*, proliferation was very poor for this sample and the cells were not evenly distributed throughout the hydrogel. Intracellular matrix production was also consistent for the PEGDA-MAETAC hydrogels, although the only sample that had obvious organized myotubular formation was the TCP group.

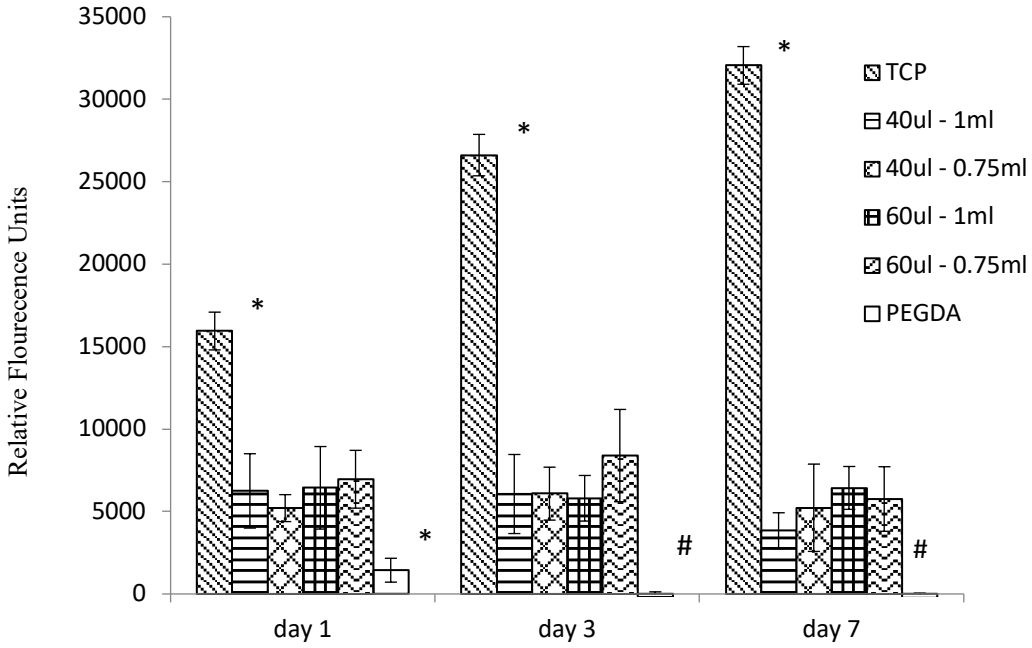

PFigure 9: Metabolic activity for C2C12 cell measured with PrestoBlue® cell viability assay. (* indicates a statistically significant difference compared to all other values with $P < 0.05$; # indicates that these two values are statistically significantly different from all other values except each other with $P < 0.05$).

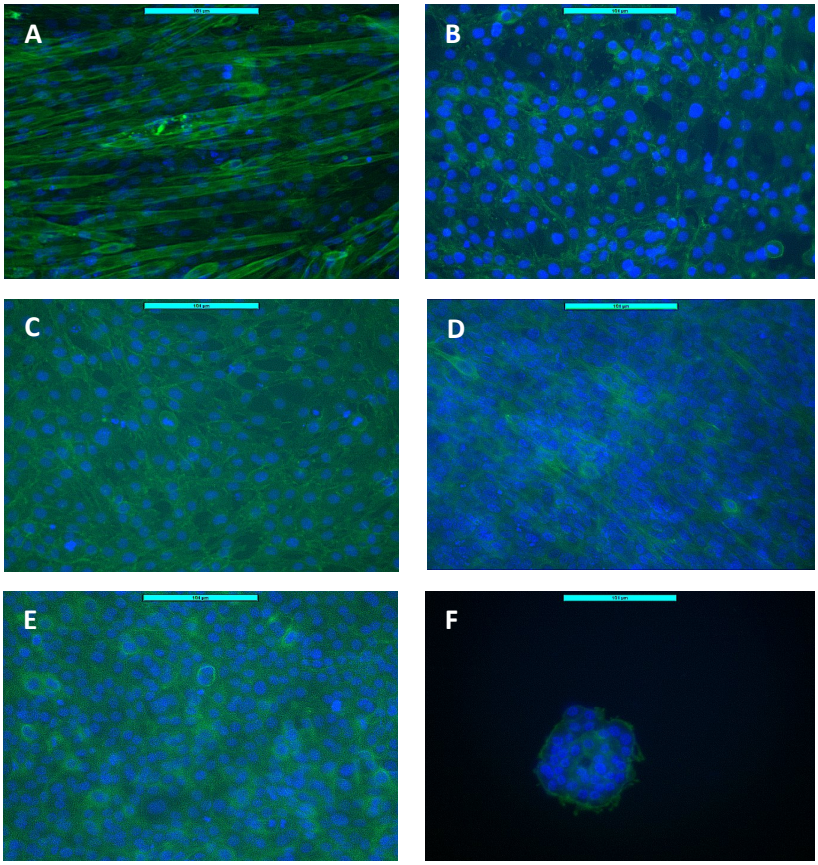

Figure 10: Cells were stained with DAPI for DNA (blue) and phalloidin for actin (green) on day 7. A) TCP, B) HS-1, C) HS-2, D) HS-3, E) HS-4, F) only PEGDA. The scale bars are all 101 µm.

2.5 Discussion

There has been very little research in the use of a positively charged hydrogel as an ionic electroactive polymer, especially for use in muscle tissue engineering. We believe the benefits could be two-fold, enhancing the proliferation and differentiation of cells, while also providing a pre-existing source of cations to be used within the hydrogel to produce the bending motion.

Since this hydrogel already contains cations, there is no need to provide an electrolyte solution from which the hydrogel can pull cations. Instead, the hydrogel can be used in

many more applications, such as *in vivo* setups, where extremely large amounts of ions are not present. One drawback to this method is that since the positive ions are bound to the matrix instead of free in solution, this may limit the range and speed of movement of the ions as compared to negatively charged hydrogels that pull positive ions in from an electrolyte solution [6].

In this study we have developed and characterized a cationic hydrogel composed of PEGDA and MAETAC for use as a self-actuating tissue engineering scaffold. The hydrogel was electrically stimulated in an actuation device and the resulting amounts of bending were measured. This actuation device was used to examine multiple formulations, polymer densities, and hydrogel geometries and determine their effects on the ability of the hydrogel to actuate. Lastly, a seven-day cell study using C2C12 mouse myoblasts was implemented to determine the biocompatibility of several formulations of the PEGDA-MAETAC hydrogel.

Actuation tests were performed to determine the response of the hydrogels to an electric field. The effects of varying the formulation of the PEGDA-MAETAC hydrogel were analyzed by varying the molecular weight of PEGDA, the amount of MAETC, the PEGDA and MAETAC concentration, and the ratio of thickness to length of the hydrogel. Varying the molecular weight of PEGDA did not have a significant change on actuation. There was only an average difference of 12° between the molecular weights of the 1000 Da, 4000 Da and 8000 Da PEGDA. The only values that exhibited a statistically significant difference were 1000Da compared 10,000 Da, where there was a difference of 28°. This may be caused by the increase in PEG molecular weight leading to an increase in hydrogel density decreasing the amount of swelling and making it more difficult for the water to

move the hydrogel. Another reason could be that the increase in molecular weight created less MAETAC per unit volume of polymer. The MAETAC crosslinks at the ends of the PEGDA molecules, therefore a smaller molecular weight allows more PEGDA molecules (and hence more MAETAC) within a specified volume. Therefore, a hydrogel with the smaller molecular weight polymer will have a larger number of bound ions to create a greater degree of movement. Varying both the PEGDA and MAETAC concentrations produced no statistical difference in degree of actuation. While the samples with 120μL of MAETAC seemed to produce the best actuation results (although not statistically significant), as the amount of MAETAC was increased, the required crosslinking times were much higher, and the integrity of the hydrogel was reduced making the sample quite difficult to handle. Thus, the hydrogel samples with lower amounts of MAETAC were used in the cell study. The changes in polymer concentration only produced a 6.7° difference in the amount of bending, and so the concentrations of 0.1 g/ml and 0.1334 g/ml were used for the cell study. Adjusting the ratios between length, width, and thickness of the hydrogel did have an effect on the amount of bending achieved. In comparing the thickness to length ratios, the sample with the smallest ratio, 0.0275, had the largest amount of movement. This is most likely because increasing the thickness causes increased stiffness which reduces the hydrogel's ability to bend.

In order to measure the contractile stress of the hydrogel, samples were suspended in PBS with increasing weights. As with the actuation test, 20 volts was applied, and the stress was calculated from the samples that were able to achieve bending. There was no significant difference between the four groups measured ranging from 120.21±14.81 Pa to

153.72±21.41 Pa. The stress values obtained were lower than those of native muscle tissue estimated to be 60 kPa - 380 kPa [12-15].

During our calculations, the actuation test results revealed a large standard error in regards to the hydrogel samples of 40, 60, 80, and 160 Microliters of MAETAC. We repeated the mentioned actuation tests numerous times to ensure that the apparent standard error is not due to testing error. Thereafter, we concluded that the errors are due to randomly distributed cations embedded within hydrogels, which are therefore the leading cause of high variability in movement of the hydrogels.

In regards to our test in deionized water, it was demonstrated that there was no statistically significant difference in the angular change of PEGDA-1000 when comparing 40 μL with 60 μL of MAETAC. There is, however, a statistical difference when comparing 80 μL samples with either of the other two samples. For our statistical analysis, we used a One-way ANOVA with a p value <0.05 followed by the Tukey's post hoc test. In samples with PEGDA-8000, the observable amount of angular movement was reduced. The statistical analysis showed significant differences when 160 μL samples were compared to 40, 60, and 80 Microliter samples of MAETAC respectively. Like PEGDA-1000 samples, the PEGDA-8000 samples with 40, 60, and 80 Microliters of MAETAC had a p value of >0.05 and are, therefore, statistically insignificant from one another.

We theorize that the higher angular movement in hydrogel samples of PEGDA-1000 can be due to the fact there are more attachment sites available for the connection of MAETAC molecules. As mentioned previously, MAETAC molecules are the source of positive charge in these hydrogels. As theorized, the increased amount of MAETAC resulted in an increased amount of angular movement during our tests.

We also noted that the angular change of our samples is significantly less when using deionized water in comparison to the samples using PBS. This shows that PBS is the superior solution to use due to the presence of excessive number of ions. We believe that the observable increase in angular movement of samples in PBS are due to ion movement from one electrode to the other. However, hydrogel angular movement in deionized water solely depends on the cations that are randomly bound to the hydrogels (limiting their number and ability to move to the oppositely charged electrode).

Finally, the biocompatibility of the hydrogels was tested by seeding four formulations of the PEGDA-MAETAC hydrogel with C2C12 mouse myoblast cells along with TCP and a PEGDA hydrogel. Metabolic activity was measured as an approximation of cell proliferation at days 1, 3, and 7. The metabolic activity of the PEGDA-MAETAC hydrogels was significantly higher than the PEGDA hydrogel. This confirms that the addition of the positive charges found in the MAETAC did have a positive effect on cellular attachment and proliferation of mouse myoblasts as was shown with endothelial cells [16], neuronal cells [10] and osteoblasts [11]. Unfortunately, the cells did not display any alignment. It is possible that this could be induced by the addition of strain as the hydrogels are actuated. We will investigate this in future work.

2.6 Conclusions

This study has investigated the creation of an actuating, positively charged scaffold consisting of a copolymer of PEGDA and MAETAC and its potential in muscle tissue engineering. We have shown that the addition of MAETAC aids in the cellular attachment and proliferation of mouse myoblast cells. In addition, the scaffold is able to actuate when electrically stimulated without the need of external ions from its environment; although the

presence of additional ions in the surrounding environment greatly enhances hydrogel actuation. This allows the scaffold to provide both electrical and mechanical stimulation to seeded cells and developing tissue. Further research is necessary to fully determine to what extent cellular proliferation and differentiation are impacted by both mechanical and electrical stimulation. This study is an important next step in the creation of a novel, actuating scaffold to be used for muscle tissue engineering.

References

1. Slaughter, B.V., et al., *Hydrogels in regenerative medicine.* Adv Mater, 2009. **21**(32-33): p. 3307-29.
2. Hunt, J.A., et al., *Hydrogels for tissue engineering and regenerative medicine.* J. Mater. Chem. B, 2014. **2**(33): p. 5319-5338.
3. Zhu, J., *Bioactive modification of poly(ethylene glycol) hydrogels for tissue engineering.* Biomaterials, 2010. **31**(17): p. 4639-56.
4. Lee, J.H., H.B. Lee, and J.D. Andrade, *Blood compatibility of polyethylene oxide surfaces.* Progress in Polymer Science, 1995. **20**(6): p. 1043-1079.
5. Alcantar, N.A., E.S. Aydil, and J.N. Israelachvili, *Polyethylene glycol-coated biocompatible surfaces.* J Biomed Mater Res, 2000. **51**(3): p. 343-51.
6. Browe, D.P., et al., *Characterization and optimization of actuating poly(ethylene glycol) diacrylate/acrylic acid hydrogels as artificial muscles.* Polymer, 2017. **117**: p. 331-341.
7. Gunn, J.W., S.D. Turner, and B.K. Mann, *Adhesive and mechanical properties of hydrogels influence neurite extension.* J Biomed Mater Res A, 2005. **72**(1): p. 91-7.
8. Schneider, G.B., et al., *The effect of hydrogel charge density on cell attachment.* Biomaterials, 2004. **25**(15): p. 3023-8.
9. Sosnik, A. and M.V. Sefton, *Poloxamine hydrogels with a quaternary ammonium modification to improve cell attachment.* J Biomed Mater Res A, 2005. **75**(2): p. 295-307.
10. Dadsetan, M., et al., *Stimulation of neurite outgrowth using positively charged hydrogels.* Biomaterials, 2009. **30**(23-24): p. 3874-81.
11. Tan, F., et al., *Fabrication of positively charged poly(ethylene glycol)-diacrylate hydrogel as a bone tissue engineering scaffold.* Biomed Mater, 2012. **7**(5): p. 055009.
12. Close, R., *DYNAMIC PROPERTIES OF FAST AND SLOW SKELETAL MUSCLES OF THE RAT DURING DEVELOPMENT.* J Physiol, 1964. **173**: p. 74-95.

13. Kanda, K. and K. Hashizume, *Factors causing difference in force output among motor units in the rat medial gastrocnemius muscle.* J Physiol, 1992. **448**: p. 677-95.
14. Lannergren, J. and H. Westerblad, *The temperature dependence of isometric contractions of single, intact fibres dissected from a mouse foot muscle.* J Physiol, 1987. **390**: p. 285-93.
15. Close, R., *Dynamic properties of fast and slow skeletal muscles of the rat after nerve cross-union.* The Journal of Physiology, 1969. **204**(2): p. 331-346.
16. Kim, S., A.E. English, and K.D. Kihm, *Surface elasticity and charge concentration-dependent endothelial cell attachment to copolymer polyelectrolyte hydrogel.* Acta Biomater, 2009. **5**(1): p. 144-51.

Chapter 3: Self-Actuating Multilayer Scaffold for Skeletal Muscle Tissue Engineering

3.1 Abstract

Electroactive polymers (EAP), which can change shape or size in response to an electrical stimulation, have been widely used in a variety of biomedical and tissue engineering applications including smart drug delivery and artificial muscles. However, approaches to design electroactive hydrogels for such purposes are often hindered due to polymers' low conductivity, which in turn requires high electrical input to induce movements resulting in a low cell viability. In this study, we aimed to reduce the input electrical stimulation while retaining hydrogel movements. To that end, we designed a multilayered poly(ethylene glycol) diacrylate (PEGDA) hydrogel modified with a highly conductive nanocomposite prepared via colloidal blending of poly(3,4 ethylenedioxythiophene):polystyrenesulfonate (PEDOT:PSS) and graphene oxide (GO). The synthesized multilayered hydrogel was then evaluated for angular movement, electrical properties, and biocompatibility with C2C12 myoblast cells.

3.2 Introduction

Skeletal muscle tissue has the ability to regenerate the lost tissue upon injury, up to a certain threshold. However, in severe injuries with large volumetric deficiencies, often greater than 20% for a particular muscle, the natural healing mechanisms fall short and require artificial interventions [1]. Muscle injuries and diseases that lead to volumetric muscle loss affect roughly 561 million individuals worldwide thus, presenting a significant economic and social burden [2]. Tissue engineering is a revolutionary field that has demonstrated promising primary steps to treat patients with large volume muscle defects

using scaffolds [3]. These scaffolds are designed to mimic the native tissue's microenvironment while promoting cellular proliferation and differentiation.

Hydrogels have been extensively studied as a potential scaffold for tissue engineering applications due to their three-dimensional polymeric network, structural, and compositional similarities to the extracellular matrix (ECM) of the native tissues. Moreover, hydrogels can be biodegradable, non-immunogenic and can also be designed to closely match the properties of the target tissue by tuning their physical and chemical properties. Function of the skeletal muscle tissue is highly dependent on the electrochemical and mechanical signaling among the neighboring cells, therefore, scaffolds intended to promote skeletal muscle regeneration should closely mimic such properties of the tissue. It has been widely known that electrical fields can potentially aid with healing of various tissues such as bone, cartilage, and skin [4, 5]. Therefore, biocompatible, electroactive, and electroconductive materials have the potential to locally stimulate the target tissue and induce cell growth.

Poly(ethylene glycol) (PEG) is one of the most widely studied polymers in the field of biomedical and tissue engineering. PEG is a hydrophilic polymer with low cellular attachment, however can be easily modified through grafting and copolymerization to enhance cellular attachment, increase its biodegradability, electroconductivity, and electroactivity [6]. PEG's low cell attachment rate can be attributed to the formation of a hydrated surface layer that inhibits the adsorption of adhesion specific proteins such as fibronectin. To improve the conductivity of the PEG hydrogels, conductive biodegradable polymers such as PEDOT:PSS can be incorporated into a PEG matrix. PEDOT:PSS can easily disperse in water, maintain its high electroconductive properties in physiological

conditions, and has been previously used to enhance bone regeneration as a possible treatment option for bone disease or trauma [7-9].

As stated earlier, EAP have the ability to change size or shape when stimulated with an electric field. This phenomenon is due to the movement of ions from one electrode to the other along with the movement of accompanying water molecules through the hydrogel. This leads to an increased swelling on one side and shrinkage on the opposite side of the hydrogel, resulting in a bending motion. Negatively charged EAPs swell in ionic solutions and attract positively charged ions. When an electricidal field is induced, these positively charged ions move the highly polar water molecules towards the negative electrode. Since movement of water molecules is linked to the presence of positive cations, therefore, a positively charged EAP may have more versatile applications. Majority of the investigated EAP's only have a single negatively charged layer, which in turn requires a strong electric field to induce bending movement. Hence, a multilayer hydrogel with a negatively charged layer surrounded by two highly conductive positively charged layers could not only increase the systems angular movement when stimulated with lower electrical field but could also increase cell attachment and viability [10].

To that end, we have developed a Self-Actuating Multilayer Scaffold (SAMS), using modified poly(ethylene glycol) diacrylate (PEGDA) hydrogels. The positively charged layers were copolymerized with 2-(methacryloyloxy) ethyl-trimethylammonium chloride (MAETAC), PEDOT:PSS, and graphene oxide (GO). The negatively charged layer was developed by copolymerization of PEGDA with acrylic acid monomers (AA). The cationic charges within MAETAC has been shown to aid in the absorption of the anionic ECM proteins [11]. Positively charged layers within the multilayer EAP system

can provide the added benefit of inherently containing positive ions, which can be attracted to the negative electrode and thus pull the water within the hydrogel to one side causing it to swell, allowing it to bend in that direction. On the other hand, having a negatively charged layer would allow for the attraction of free-flowing cations in the solution. These free-flowing cations would move the water molecules towards the negative electrode upon stimulation with an electric field. Therefore, a multilayer hydrogel system with different charges associated to different layers can take advantage of the benefits associated with each layer. In this study, we explored the effects of SAMS on myoblast attachment and examined the applicability of the multilayer scaffold with either both negative or positive layers for potential use in muscle tissue engineering.

3.3 Experimental Section

3.3.1 Materials

All the materials used in this study were purchased from Sigma Aldrich with the following exceptions. Poly(ethylene glycol) diacrylate (PEGDA) with molecular weight of 8000 kDa was purchased from Monomer Polymer & Dajac Labs. Dapi and Fluorescein Phalloidin were purchased from Thermo Fisher. PEDOT:PSS was purchased as a 1.1% dispersion in water with a neutral pH.

3.3.2 PEDOT:PSS/GO Nanocomposite Film Fabrication

Graphene oxide (GO) was prepared using Hummer's method by mixing H_2SO_4, H_3PO_4, graphite flakes, and $KMnO_4$ for three days. Mixture was later purified and dried in the oven [12]. As PEDOT:PSS tends to aggregate at high temperatures, solution was sonicated for one hour prior to use [13]. PEDOT:PSS was mixed with DMSO and EG at 5% and 6% (v/v) respectively. GO at 6% (wt/wt) was dispersed in DMF via sonication at

room temperature before being added to the PEDOT:PSS mixture. PEDOT:PSS/GO mixture was further sonicated until a homogenous dispersion was achieved. The mixture was casted onto a nonstick paper and dried in a hot air oven at 75°C for 10 hours followed by 1 hour at 150°C in a vacuum chamber to ensure complete solvent evaporation. PEDOT:PSS/GO nanocomposites were then peeled off and used for further experimentation and hydrogel synthesis.

3.3.3 Self-Actuating Multilayer Scaffold (SAMS) Fabrication

SAMS is made of three layers of hydrogel. Inner hydrogel layer was formed by dissolving PEGDA and acrylic acid monomer (AA) in phosphate buffer saline (PBS, pH=7.4) [14]. The photo-initiator solution of 300 mg/mL of 2,2-dimethoxy-2-phenyl acetophenone in 1-vinyl-2-pyrrolidinone was prepared using a vortex mixer. The photo-initiator solution was added just prior to applying ultraviolet (UV) radiation at a concentration of 100 μL of photo-initiator solution per 1 mL of hydrogel solution (10% v/v). The hydrogel solution was then injected into a rectangular glass mold and cross-linked with UV radiation at a wavelength of 365 nm and intensity of 10 W for 2 minutes. As depicted in *Figure 1,* hydrogels samples were then placed in a PBS bath to swell and achieve equilibrium for 24 hours. The samples were cut into 20 mm x 5 mm samples and dried overnight in an oven at 50°C. When samples were fully dried, they were rehydrated overnight in 20 ml of 1:8 PEGDA:AA solution.

The two identical outer layers were formed by dissolving PEGDA into deionized (DI) water using a vortex mixer. Based on the previously established protocol, 60 ul of MAETAC per 0.1g of PEGDA was then added and vortexed until sufficiently mixed [15]. Various amounts of pre-prepared PEDOT:PSS/GO nanocomposite film was added and the

solution was left to sonicate until a homogenous mixture was achieved. Photo-initiator solution, with the same concentration as above, was added just prior to applying UV radiation. Hydrogel solution was then injected into a glass mold to fully cover the PEGDA:AA hydrogel and cross-linked with UV radiation at a wavelength of 365 nm and intensity of 10 W for 2 minutes. Final thickness of the SAMS was 1.27±0.04 mm. The glass mold was flipped every 20 seconds to ensure an even coverage of PEGDA/MAETAC/PEDOT:PSS/GO hydrogel. Newly prepared SAMS were then placed in PBS for one hour and cut again to be 20 mm x 5 mm before actuation.

All PBS used in this study was prepared by mixing 2.455 g/L sodium phosphate dibasic heptahydrate, 8.765 g/L sodium chloride, and 0.138 g/L monosodium phosphate in 1 liter of deionized water with the final pH of 7.4.

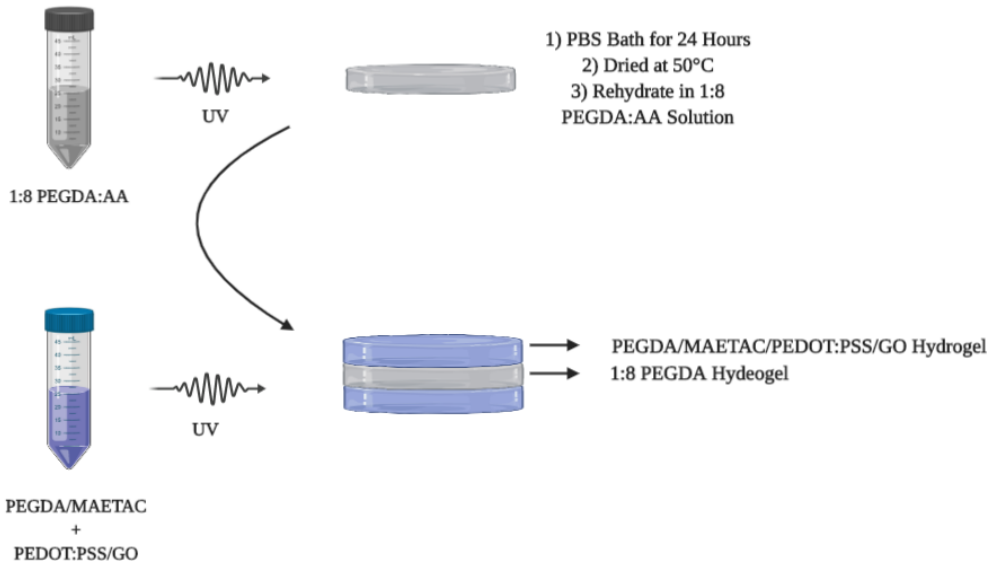

Figure 5 Graphical depiction of SAMS fabrication and photopolymerization of the precursor solutions to form hydrogel. Highly conductive PEDOT:PSS/GO nanocomposite are incorporated in the outer layers of SAMS. Conductive layer would allow for transfer of charge and to induce movement at a low applied voltage. Inner layer of is made of 1:8 PEGDA:AA hydrogel.

3.3.4 Conductivity and Electrochemical Impedance Spectroscopy (EIS)

Nanocomposites films were cut into 1 cm x 1 cm pieces. After application of a DC voltage of 3 V (n=4), the current output was recorded. Conductance was later calculated using the following equation, where conductance is C, current is I, voltage is V, and cross-sectional area of the nanocomposite film is represented as A. Power supply used to measure conductivity was E3646A dual output DC (Agilent Technologies, Santa Clara, CA).

$$C = \frac{L}{\left(\frac{V}{I}\right) * A}$$

Hydrogels were swollen in deionized water overnight at room temperature and the water was replaced twice to remove any possible salt residues. Hydrogel samples were weighted, and 0.5 grams were used to fill one well of a 12-well plate. Electrodes were previously fixed to the sides of the well at the furthest point from one another. Measurements were recorded between 0 and 100 Hz with an AC amplitude of ±50 mV.

3.3.5 Contact Angle

Contact angle measurements were undertaken to measure the water-film interactions. An increase in the contact angle can be representative of an increase in the film's hydrophobicity. To measure the contact angle, the previously fabricated nanocomposite films were mounted on a stand. Following the mounting, 50 μL of deionized water was added on top of the films and imaged using a digital camera mounted on the same plane. Images were processed using Image J software.

3.3.6 Actuation Testing

As previously mentioned, all hydrogel samples were cut into 20 mm x 5 mm and stored in PBS prior to testing. Testing apparatus, as depicted in *Figure 2*, was designed to create an electrode-hydrogel contact at the center of the hydrogel sample. All tests were

performed in PBS with n=4. Electrodes used were 99.5% pure platinum wires with a diameter of 0.20-mm. Electrodes were attached to an Agilent Dual Output DC Power Supply (E3646A Agilent Technologies, Santa Clara, CA, USA). The polarity was switched every minute for a total of 5 minutes. Sample movements were recorded and analyzed for angular movement.

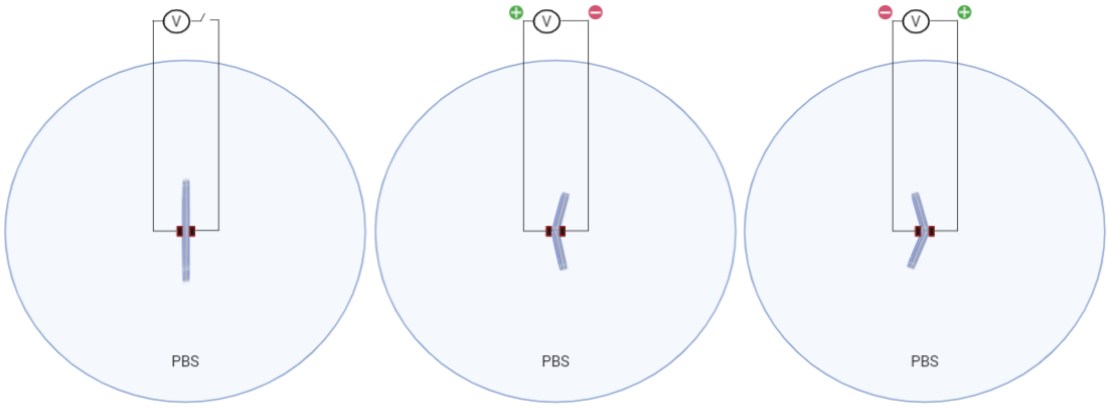

Figure 6 Schematic of the device used for actuation testing of the multilayer conductive PEDOT-PEGDA hydrogel samples. A) System at rest with no current. B&C) Hydrogel samples are stimulated and moving due to transfer of ions as the polarity changes representing forward and reverse movements.

3.3.7 C2C12 Cytotoxicity Study

PEGDA/MAETAC and nanocomposite samples, n=6, were prepared and cut into circles with a diameter of 15mm. Samples were then placed in low attachment 24-well culture plates. Each side of the samples was treated with 30 minutes of UV and then washed with 70% ethanol. Samples were further washed with sterile PBS and were incubated overnight at 37°C in Dulbecco's Modified Eagle Medium (DMEM) with 10% fetal bovine serum (FBS), and 1% penicillin/streptomycin (P/S). Wells were then seeded on day 0 with C2C12 mouse myoblast cells at a 60,000 cells per well (30,000 cells/cm^2).

To assess sample biocompatibility, PrestoBlue cell viability assay was used to measure cells metabolic activity and cellular proliferation on 1 and 3 days after seeding.

During these time points, cells were incubated for one hour with DMEM media and 10% PrestoBlue. Absorbance was later measured using a Tecan Infinite M200 PRO plate reader at 570 nm. On Day 3, cells were fixed using 4% paraformaldehyde solution and stained with DAPI and Fluorescein Phalloidin for DNA and F-actin, respectively.

3.3.8 X-ray Photoelectron Spectroscopy (XPS)

Thermo Scientific K-Alpha equipped with a monochromated Al Kα x-ray source with an energy of 1486.6 eV and total energy resolution of 0.5 eV was used to preform XPS measurements. Charge compensation was performed to minimize electrical charge buildup during XPS measurements by using a dual beam flood source of low-energy Ar+ ions and 1 eV electrons. Finally, by subtracting Shirley backgrounds and then fitting the remaining core level features with Voigt profile components, the XPS spectra was analyzed. XPS was used to quantify the atomic ratio of carbon to oxygen (C/O) of GO and further evaluate this substance electrical conductivity.

3.3.9 Statistics Analysis

The average and standard deviation of the data for each group were calculated. All data were evaluated with a one-way ANOVA with a Tukey's post-hoc test and significance was set at $\alpha = 0.05$ (denoted by *).

3.4 Results and Discussion

3.4.1 The effect of varying GO concentration in nanocomposite hydrophilicity

Due to GO's high number of hydroxyl and epoxy functional groups, this substance was used to increase hydrophilicity of the PEDOT:PSS and further enhance nanocomposite attachment to the hydrogel. As shown in *Figure 3*, contact angle is significantly increased from 41.5° to 90° as the concentration of GO was reduced and PEDOT:PSS was increased.

3.4.2 Electrical conductivity

Conductivity of PEDOT:PSS/GO nanocomposite films were measured prior to their incorporation within the SAMS system. Conductivity of the PEDOT:PSS/GO nanocomposite films were recorded to be 55 S/cm while GO was 0 S/cm (*Figure 4)*. Due to the disruption in the sp2 bonding network, GO is a considered to be a great insulator and was used in small increments to increase PEDOT:PSS hydrophilicity. Hydroxyl and epoxy functional groups attached to the sp3 hybridized carbons in GO accounts for the highly hydrophilic nature. XPS survey of the GO samples were performed and by calculating the area under the curve, we quantified the atomic ratio of carbon to oxygen (C/O) to be 2.45, further reduction beyond C/O of 6 may have increased its conductivity.

As mentioned, ion transport within native tissue occurs in an altering, bidirectional, and at a wide range of frequencies [19]. Therefore, to better measure the conductivity of SAMS, we used electrochemical impedance spectroscopy (EIS). EIS measures electron transfer from capacitive and resistive effects, which can more closely mimic the ion transport within the native tissue. As depicted in *Figure 5,* an increase in frequency yielded similar and low impedance measurements for all samples, which may be attributed to capacitive currents within samples. On the other hand, at the lower end of the frequency similar to that of the native tissue, spectrum resistive current dominates. Based on our measurements, impedance was significantly reduced from 540 to 226, 280, and 249 kOhm at 1.5 Hz for SAMS samples containing 0%, 10%, 20%, and 30%, respectively, of PEDOT:PSS/GO nanocomposites. Thus, we can conclude that PEDOT:PSS/GO has significantly enhanced electroconductivity of SAMS samples.

3.4.3 The Effect of Varying the Applied Potential Difference on Angular Movement

In regard to our actuation test under 1 volt, it was demonstrated that the movement of the SAMS groups were significantly enhanced with the addition of the conductive layers in comparison to the 0% control group. For our statistical analysis, we used a One-way ANOVA with a p-value <0.05 followed by the Tukey's post hoc test. Regarding our tests under 5 and 10 volts, although the overall trend seems to show that the addition of the conductive layer increased sample movement, but only a few groups showed a statistical difference with their corresponding 0% control groups. Similarly, there was no statistical difference between the 10%, 20%, and 30% groups demonstrating a p-value of >0.05 Figures 6-8.

We noted that increased applied voltage to the SAMS groups resulted in significant increase in the hydrogel movement and angular speed. We believe that the observable increase in angular movement of samples in PBS, from less than 10 degrees in 1V to more than 150 degrees in 10V are due to the increased ion movement from one conductive layer to the other.

3.4.4 C2C12 Cytotoxicity Study

Biocompatibility of the GO, PEDOT:PSS, and PEDOT:PSS/GO nanocomposite films was compared with PEGDA-MAETAC hydrogels incorporating different concentrations of 0, 10, 20, and 30% of PEDOT:PSS/GO nanocomposite. As seen in *Figure 10*, cell proliferation and metabolic activity was measured on day 1 and 3. All four PEGDA-MAETAC hydrogel samples (0%, 10%, 20%, and 30%) are significantly more biocompatible than the nanocomposites films. When comparing the hydrogel samples with

one another, 0 and 10% PEDOT:PSS/GO samples are significantly more biocompatible than 20 or 30% PEDOT:PSS/GO samples. As can be seen in *Figure 11*, cell proliferation was very low for 20% samples in comparison with 0 and 10% hydrogel samples.

The metabolic activity of the 30%, 20%, and 10% were lower than the PEGDA-MAETCA hydrogel. This confirms that the addition of the PEDOT:PSS has a negative effect on cellular attachment and proliferation of mouse myoblasts.

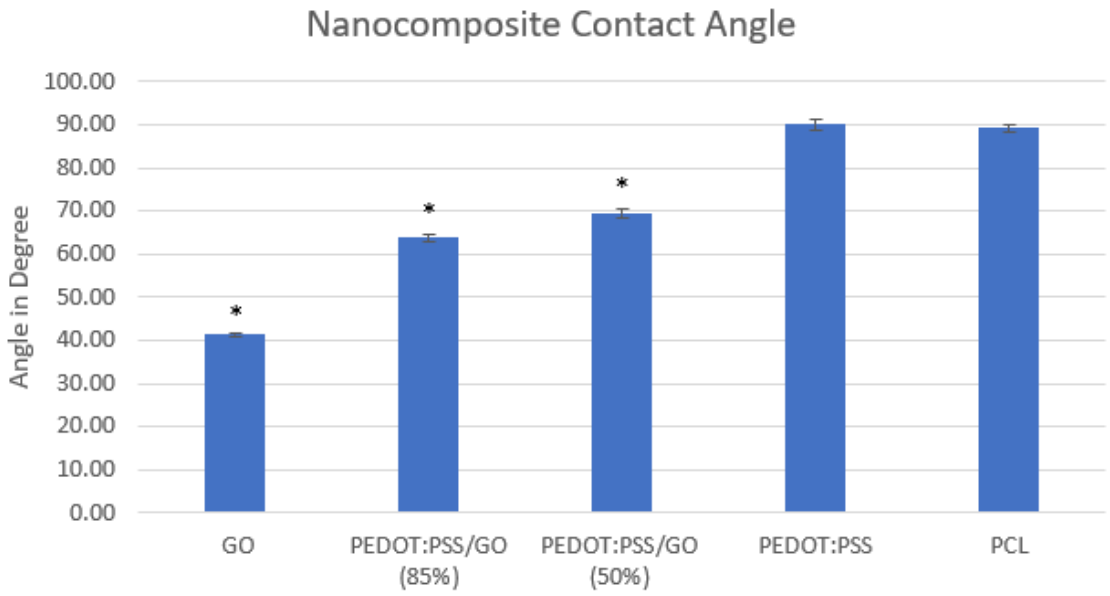

Figure 7 Contact angle measured to compare the effects of varying amount of GO in PEDOT/GO nanocomposite films. Polycaprolactone (PCL) was used as hydrophobic control. Contact angle is measured in degrees (indicates a statistically difference with P< 0.05, compared to PEDOT:PSS sample). This finding indicates that an increase in the amount of GO is correlated with an increased in hydrophilicity of the nanocomposite films.*

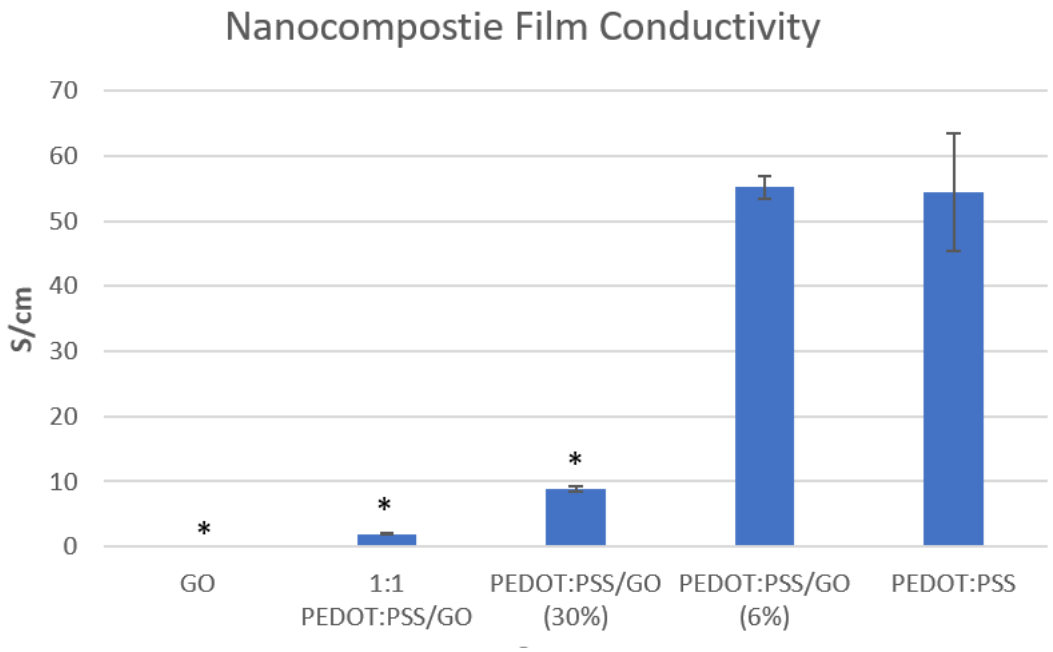

Figure 8 Nanocomposite films conductivity with different concentration of GO is measured (n=4). This finding indicates that as concentration of GO decreases conductivity of the nanocomposite films increase. Conductivity is measured in S/cm (indicates a statistically difference with P< 0.05, compared to PEDOT:PSS sample).*

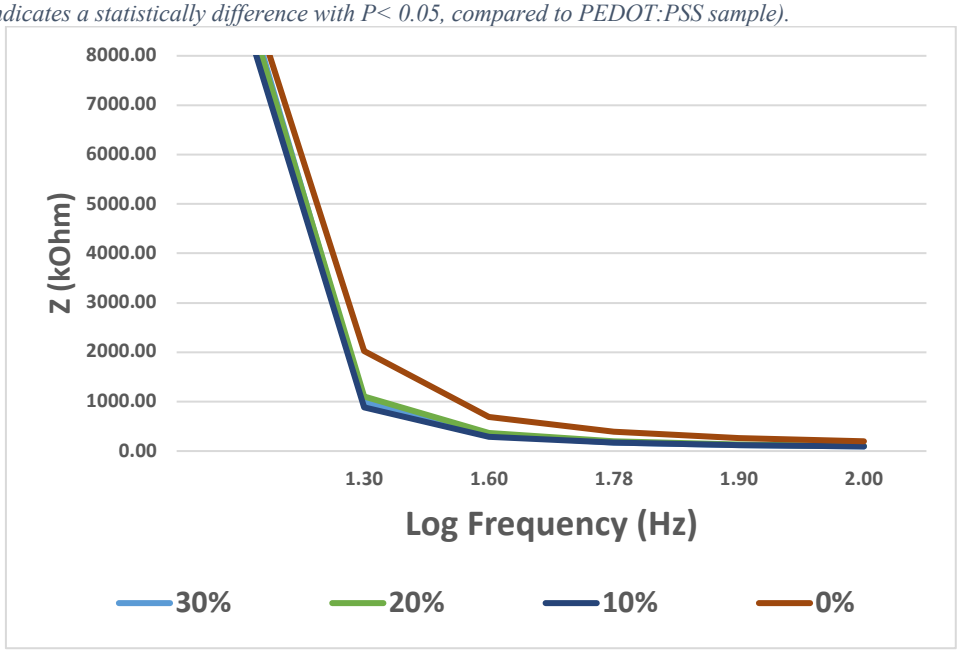

Figure 9 Electrochemical impedance spectroscopy (EIS) measurements of the hydrogel samples with varying amount of PEDOT/GO nanocomposite concentration.

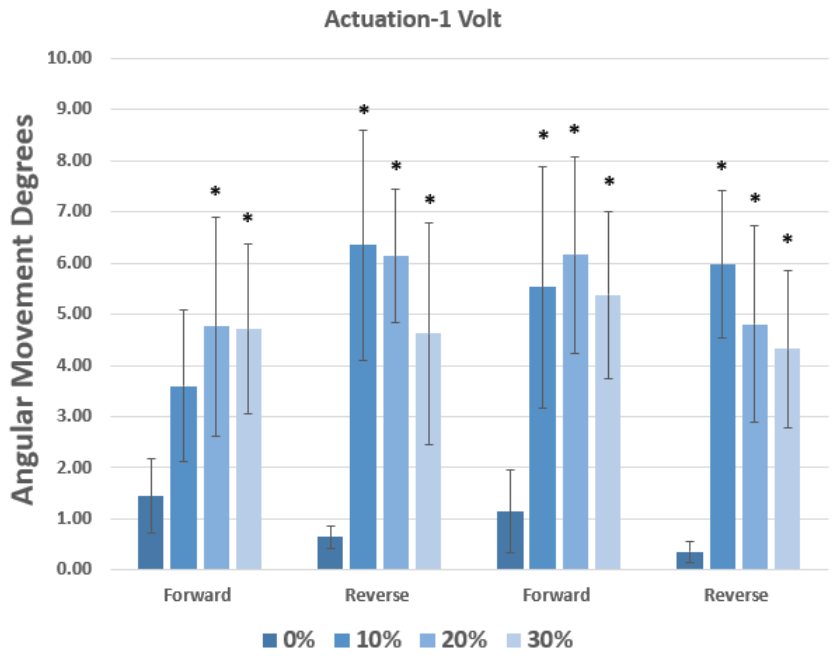

Figure 10 Effects of varying amount of PEDOT/GO nanocomposite embedded within the outer layer of the hydrogel samples on angular movement(n=4) with an applied voltage of 1V. Forward and reverse movements are depicted for each group. (indicates a statistically difference with the 0% group, which is PEGDA-MAETAC with no added PEDOT:PSS/GO).*

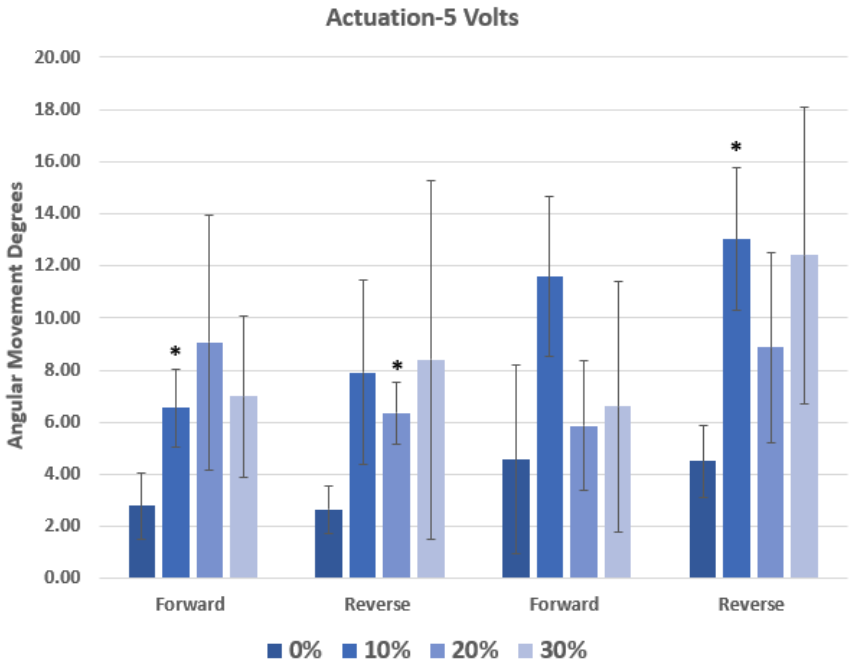

*Figure 11 Effects of varying amount of PEDTO/GO nanocomposite embedded within the outer layer of the hydrogel samples on angular movement(n=4) with an applied voltage of 5V. Forward and reverse movements are depicted for each group. * indicates a statistically difference with 0% group.*

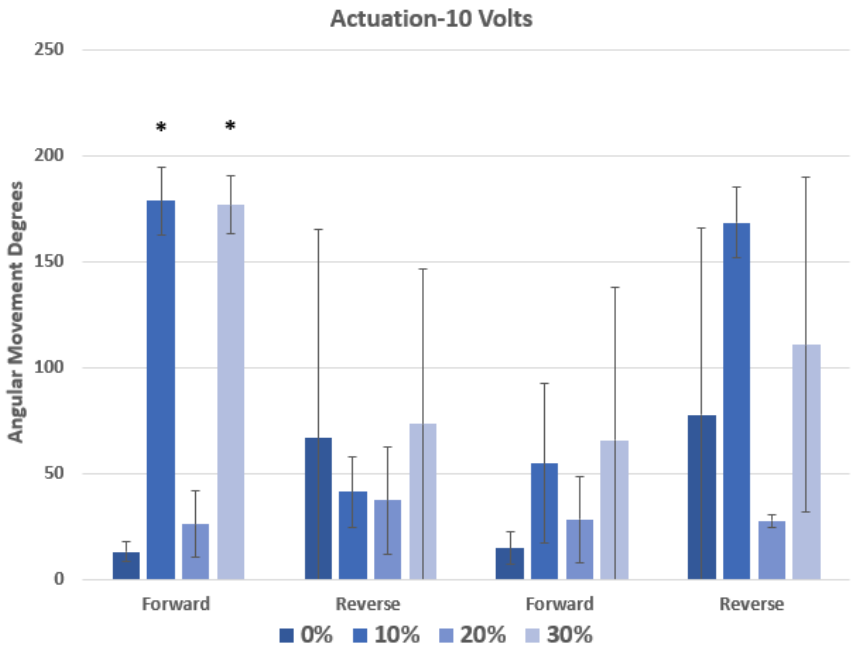

*Figure 12 Effects of varying amount of PEDTO/GO nanocomposite embedded within the outer layer of the hydrogel samples on angular movement(n=4) with an applied voltage of 10V. Forward and reverse movements are depicted for each group. * indicates a statistically difference with 0% group.*

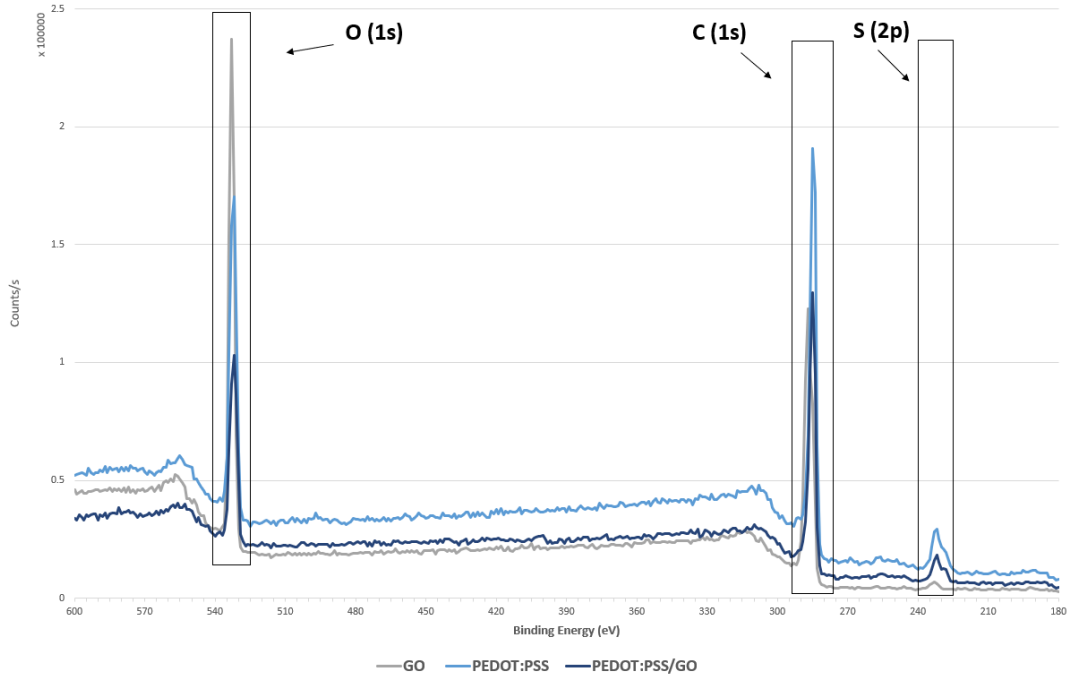

Figure 13 X-Ray Photon Spectroscopy of the three nanocomposite samples of GO, PEDOT:PSS, and PEDOT:PSS/GO. The first peak represents O(1s), second peak represents C(1s) and the last peak is S(2p), which corresponds to the sulfur in PEDOT:PSS.

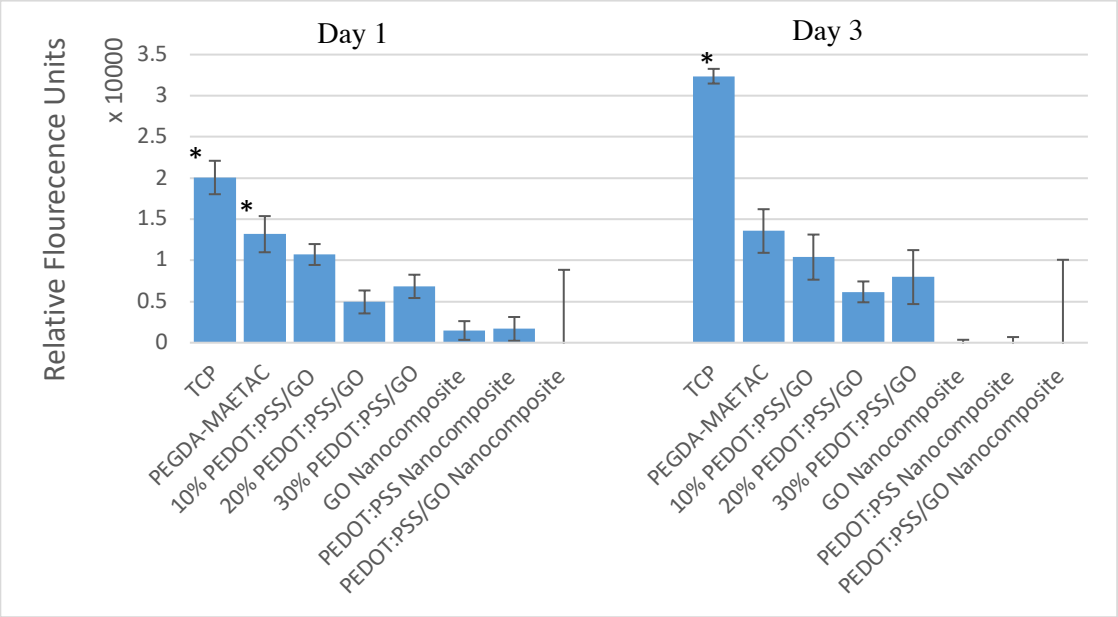

Figure 14 Metabolic activity for C2C12 cell measured with PrestoBlue® cell viability assay. (indicates a statistically significant difference compared to all other values with P< 0.05).*

3.4.5 Discussion

Applications of multilayered actuating hydrogels for skeletal muscle tissue engineering scaffolds are very limited. PEGDA-based electroactive hydrogels have been previously developed in our laboratory for skeletal muscle tissue engineering purposes [3, 4]. Herein, we have developed a SAMS, consisting of two highly conductive and positively charged PEGDA/MAETAC/PEDOT/GO outer layers and 1:8 PEGDA:AA inner layer (*Figure 1)*. We believe that the development SAMS is the first step towards enhancing the proliferation and differentiation of myoblasts to myotubes. One drawback of this system is the increased scaffold thickness due to the incorporation of several layers. Increased thickness of the scaffold can restrict the bending motion. In this study, SAMS was electrically stimulated to measure the bending motion of the scaffold. Bending motion measurements are used to study the effects of various formulation of the SAMS's

conductive layer. Lastly, a three-day cell study using C2C12 mouse myoblasts was implemented to examine the biocompatibility of several formulations of the SAMS's conductive layer.

Traditionally, the use of actuating hydrogels was limited to *in-vitro* applications. This limitation can be attributed to two major reasons; 1) in order to achieve a considerable bending motion, a high electrical field was required leading to reduced cell viability, and 2) hydrogel swelling brings about a great stress to any attached material, causing failure at the interface and detachment. To that end, SAMS was developed to address these shortcomings. SAMS's conductive layers can greatly reduce the distance between two poles and exert the needed electrical field at a safer and more tolerable potential difference. Also, every layer used in SAMS is a different modification of PEGDA hydrogel, therefore, the swelling motion is experienced at the similar rate throughout the scaffold leading to a reduction of stress at the interface.

It has been previously reported that the addition of solvents such as DMSO and EG could significantly enhance the electrical conductivity of PEDOT:PSS nanocomposite films [16]. Although there has been no definitive reason for such drastic electrical conductivity enhancement, some believe that this could be due to screening effects and reduction in PSS interactions. DMSO, a polar solvent in nature, could induce a screening effect between the charge carriers and the counter ions, which results in reducing the point charge interactions between negatively charged PSS and positively charged PEDOT. Similarly, EG has been reported to effect and reduce the interaction of PSS with PEDOT. Such mechanism could potentially explain the increase in nanocomposite films electrical conductivity [17, 18]. statistical difference between the 10%, 20%, and 30% SAMS groups

(p-value of >0.05). Therefore, indicating that in future work 10% samples are not only more biocompatible but provide sufficient angular movement. The 10% SAMS samples could be a candidate to electrically and mechanically stimulate cells. To further improve cell attachment and biocompatibility we will investigate the incorporation of cell adhesion peptide arginine–glycine–aspartic acid (RGD) in future work.

During our calculations, the actuation test results revealed a large standard error regarding the SAMS samples of 0%, 10%, 20%, and 30%. We repeated the mentioned actuation tests numerous times to ensure that the apparent standard error is not due to testing error. Thereafter, we concluded that the errors are due to the sample deformation at the SAMS/platinum electrode contact site, which results in discontinuous electron flow to the conductive layer.

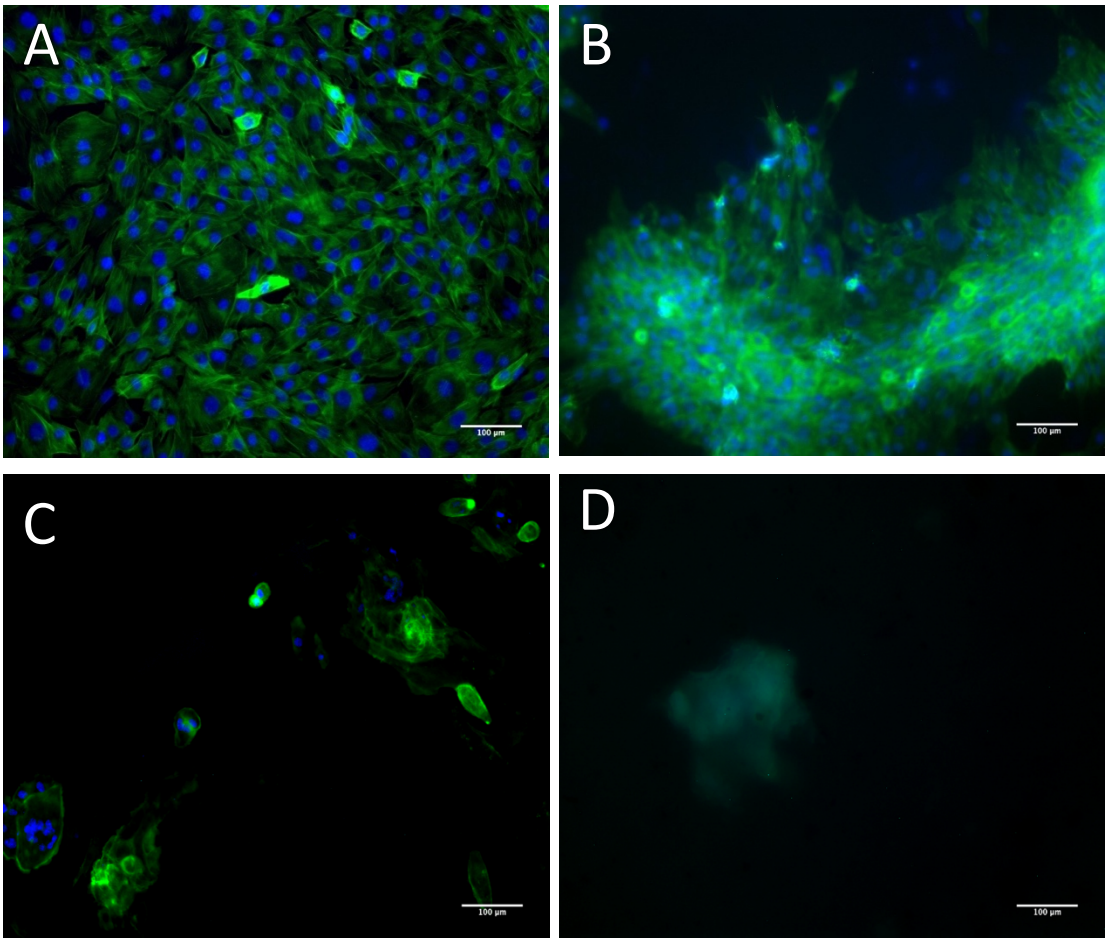

Figure 15 Cells were stained with DAPI for DNA (blue) and phalloidin for actin (green) on day 3. A) Untreated control, B) 0% PEDOT:PSS/GO nanocomposite, C) 10% PEDOT:PSS/GO nanocomposite, and D) 20% PEDOT:PSS/GO nanocomposite. The scale bars are all 100 µm.

3.5 Conclusion

We have successfully developed a multilayer actuating hydrogel scaffold through the use of highly conductive PEDOT:PSS and copolymer of PEGDA and MAETAC. It was found that embedding conductive polymers within the outer layer of the multilayer construct would not only stabilize but also increase movements, which may provide further insights in differentiation and proliferation of myocytes into functional muscle tissue. In

addition, this multilayered scaffold actuates to a much higher degree in comparison to our previously developed models with a low electrical stimulation, which may translates into higher cell viability and greater exerted contractile force. This scaffold is suitable to provide both electrical and mechanical stimulation to develop complex tissues including skeletal muscle. This study has demonstrated an important next step in development of novel and complex soft multilayer actuators for skeletal muscle tissue engineering purposes. However, further research is needed to study proliferation and differentiation of myotubes under electrical and mechanical stimulation for understanding regenerative potential of skeletal muscle tissue.

References

1. Jarvinen, T.A.H., et al., *Muscle injuries: optimising recovery.* Best Practice & Research in Clinical Rheumatology, 2007. **21**(2): p. 317-331.
2. Manring, H., et al., *Novel excitation-contraction coupling related genes reveal aspects of muscle weakness beyond atrophy-new hopes for treatment of musculoskeletal diseases.* Frontiers in Physiology, 2014. **5**.
3. Lee, K.Y. and D.J. Mooney, *Hydrogels for tissue engineering.* Chemical Reviews, 2001. **101**(7): p. 1869-1879.
4. Slaughter, B.V., et al., *Hydrogels in Regenerative Medicine.* Advanced Materials, 2009. **21**(32-33): p. 3307-3329.
5. Hunt, J.A., et al., *Hydrogels for tissue engineering and regenerative medicine.* Journal of Materials Chemistry B, 2014. **2**(33): p. 5319-5338.
6. Alcantar, N.A., E.S. Aydil, and J.N. Israelachvili, *Polyethylene glycol-coated biocompatible surfaces.* Journal of Biomedical Materials Research, 2000. **51**(3): p. 343-351.
7. Khan, S., et al., *Synthesis and characterization of a novel bacterial cellulose–poly(3,4-ethylenedioxythiophene)–poly(styrene sulfonate) composite for use in biomedical applications.* Cellulose, 2015. **22**: p. 2141-2148.
8. Thaning, E.M., et al., *Stability of Poly(3,4-ethylene dioxythiophene) Materials Intended for Implants.* Journal of Biomedical Materials Research Part B-Applied Biomaterials, 2010. **93B**(2): p. 407-415.
9. Shahini, A., et al., *3D conductive nanocomposite scaffold for bone tissue engineering.* International Journal of Nanomedicine, 2014. **9**: p. 167-181.
10. Geng, T., et al., *Flow-through electroporation based on constant voltage for large-volume transfection of cells.* Journal of Controlled Release, 2010. **144**(1): p. 91-100.
11. Tan, F., et al., *Fabrication of positively charged poly(ethylene glycol)-diacrylate hydrogel as a bone tissue engineering scaffold.* Biomedical Materials, 2012. **7**(5).
12. Huang, N.M., et al., *Simple room-temperature preparation of high-yield large-area graphene oxide.* International Journal of Nanomedicine, 2011. **6**: p. 3443-3448.
13. Zhou, J., et al., *The temperature-dependent microstructure of PEDOT/PSS films: insights from morphological, mechanical and electrical analyses.* Journal of Materials Chemistry C, 2014. **2**(46): p. 9903-9910.
14. Browe, D.P., et al., *Characterization and optimization of actuating poly(ethylene glycol) diacrylate/acrylic acid hydrogels as artificial muscles.* Polymer, 2017. **117**: p. 331-341.
15. Scott, T.E., et al., *Characterization and optimization of a positively charged poly (ethylene glycol)diacrylate hydrogel as an actuating muscle tissue engineering scaffold.* Polymers for Advanced Technologies.
16. Takano, T., et al., *PEDOT Nanocrystal in Highly Conductive PEDOT:PSS Polymer Films.* Macromolecules, 2012. **45**(9): p. 3859-3865.
17. Okuzaki, H., Y. Harashina, and H. Yan, *Highly conductive PEDOT/PSS microfibers fabricated by wet-spinning and dip-treatment in ethylene glycol.* European Polymer Journal, 2009. **45**(1): p. 256-261.

18. Kim, J.Y., et al., *Enhancement of electrical conductivity of poly(3,4-ethylenedioxythiophene)/poly(4-styrenesulfonate) by a change of solvents.* Synthetic Metals, 2002. **126**(2-3): p. 311-316.
19. Breukers, R.D., et al., *Creating conductive structures for cell growth: Growth and alignment of myogenic cell types on polythiophenes.* Journal of Biomedical Materials Research Part A, 2010. **95A**(1): p. 256-268.